Received: 21 June 2019 | Revised: 27 July 2019 | Accepted: 30 July 2019

DOI: 10.1002/cne.24752

RESEARCH ARTICLE

JCN RESEARCH IN SYSTEMS NEUROSCIENCE THE JOURNAL OF COMPARATIVE NEUROLOGY WILEY

Mushroom bodies in Reptantia reflect a major transition in crustacean brain evolution

Nicholas J. Strausfeld[1] | Marcel E. Sayre[2]

[1]Department of Neuroscience, School of Mind, Brain and Behavior, University of Arizona, Tucson, Arizona

[2]Lund Vision Group, Department of Biology, Lund University, Lund, Sweden

Correspondence
Nicholas J. Strausfeld, Department of Neuroscience, School of Mind, Brain and Behavior, University of Arizona, Tucson, Arizona.
Email: flybrain@neurobio.arizona.edu

Funding information
National Science Foundation, Grant/Award Number: 175479

Abstract

Brain centers possessing a suite of neuroanatomical characters that define mushroom bodies of dicondylic insects have been identified in mantis shrimps, which are basal malacostracan crustaceans. Recent studies of the caridean shrimp *Lebbeus groenlandicus* further demonstrate the existence of mushroom bodies in Malacostraca. Nevertheless, received opinion promulgates the hypothesis that domed centers called hemiellipsoid bodies typifying reptantian crustaceans, such as lobsters and crayfish, represent the malacostracan cerebral ground pattern. Here, we provide evidence from the marine hermit crab *Pagurus hirsutiusculus* that refutes this view. *P. hirsutiusculus*, which is a member of the infraorder Anomura, reveals a chimeric morphology that incorporates features of a domed hemiellipsoid body and a columnar mushroom body. These attributes indicate that a mushroom body morphology is the ancestral ground pattern, from which the domed hemiellipsoid body derives and that the "standard" reptantian hemiellipsoid bodies that typify Astacidea and Achelata are extreme examples of divergence from this ground pattern. This interpretation is underpinned by comparing the lateral protocerebrum of *Pagurus* with that of the crayfish *Procambarus clarkii* and *Orconectes immunis*, members of the reptantian infraorder Astacidea.

KEYWORDS

evolution, hemiellipsoid body, homology, mushroom body, Pancrustacea, Reptantia, RRID: AB_572263, RRID:AB_1157911, RRID:AB_1566510, RRID:AB_301787, RRID:AB_477,019, RRID:AB_528479, RRID:AB_572268

1 | INTRODUCTION

Mushroom bodies are paired association centers in the lateral protocerebra of insects (review: Farris & Van Dyke, 2015), which in certain species have been demonstrated to assess stimulus valences and support memory formation (Cognigni, Felsenberg, & Waddell, 2018). They are denoted by their columnar neuropils comprising hundreds, in some species many thousands, of intrinsic neurons, called Kenyon cells, arranged as parallel fibers extending from clusters of extremely small basophilic cell bodies, called globuli cells. Arborizations of input and output neurons intersect parallel fibers down the length of the columns. And, in most insect species, dendrites belonging to intrinsic neurons provide a distal cap-like neuropil, called the calyx, from which the columns extend. Generally, the calyx receives its major input from relay neurons carrying information from olfactory neuropils in the deutocerebrum, but other modalities are also represented in the calyces of many insect species (Farris & Sinakevitch, 2003; Gronenberg, 2001; Vogt, Aso, Hige, Knapek, Ichinose, & Friedrich, et al., 2016).

Of particular diagnostic value for identifying centers that possess characters typifying insect mushroom bodies is an antibody called DC0 that recognizes the catalytic subunit of protein kinase A (Kalderon & Rubin, 1988). Anti-DC0 selectively resolves the columnar neuropils of mushroom bodies across insect species (Farris &

Strausfeld, 2003) and of corresponding protocerebral centers in many other arthropod lineages (Wolff, Harzsch, Hansson, Brown, & Strausfeld, 2012; Wolff & Strausfeld, 2015). This affinity to anti-DC0 may be an indicator of shared functionality across these centers in that DC0 is required for effective learning and memory attributed to the mushroom bodies of *Drosophila* (Skoulakis, Kalderon, & Davis, 1993).

The selective affinity of anti-DC0 extends to the columnar mushroom body lobes of Stomatopoda and Caridea, both of which are malacostracan crustaceans (Wolff, Thoen, Marshall, Sayre, & Strausfeld, 2017; Sayre & Strausfeld, 2019). However, instead of possessing columnar centers in their lateral protocerebra, the reptantian infraorders Achelata and Astacidea have approximately dome-shaped centers called hemiellipsoid bodies (Blaustein, Derby, Simmons, & Beall, 1988; Sullivan & Beltz, 2001a, 2001b). As demonstrated by a pioneering study in 1968 (Maynard & Yager, 1968), hemiellipsoid bodies and the lateral protocerebra are crucial in olfactory processing and eliciting odor-induced behaviors (Mellon, 2000; Mellon, 2003). In addition, studies of hemiellipsoid body development using tract tracing methods have demonstrated that these centers are much more than higher olfactory processors, but are connected to numerous parts of the lateral protocerebrum to which they supply outputs or from which they receive information (Sullivan & Beltz, 2001b). Hemiellipsoid bodies occupy locations in the brain corresponding to the locations occupied by the mushroom bodies in the lateral protocerebra of insects, as well as of stomatopods and caridean shrimps (Wolff et al., 2017; Sayre & Strausfeld, 2019). Like mushroom bodies, hemiellipsoid bodies receive inputs from deutocerebral olfactory neuropils and can, as will be show here, express elevated levels of DC0. However, despite the identification of mushroom bodies in malacostracans that are outgroups of decapods, contemporary accounts of decapod brains nevertheless define hemiellipsoid bodies as crustacean apomorphies and state, categorically, that these structures are established elements of the cerebral ground pattern of Malacostraca (Kenning, Müller, Wirkner, & Harzsch, 2013; Wittfoth, Harzsch, Wolff, & Sombke, 2019).

What is more plausible—a ground pattern organization referring to columnar mushroom bodies as resolved in Stomatopoda, an outgroup of Decapoda, or domed centers typifying reptantian decapods? Might the reptantian hemiellipsoid body be the homologue of the columnar mushroom body and, if so, what evidence would support this?

The original proposition that hemiellipsoid bodies may be highly modified mushroom bodies (Strausfeld, Buschbeck, & Gomez, 1995; Strausfeld, Hansen, Li, Gomez, & Ito, 1998) has found support from neuroanatomical studies of these centers in the Bermuda hermit crab *Coenobita clypeatus*, belonging to an evolutionarily young lineage of Anomura (Bracken-Grissom et al., 2013; Wolfe et al., 2019; Wolff et al., 2012). In *C. clypeatus*, the hemiellipsoid bodies are composed of stratified arrangements of DC0-immunopositive laminae that contain orthogonally arranged circuits, which, like those of mushroom body columns, comprise intrinsic neuron processes intersected by the dendrites and terminals of extrinsic neurons (Brown & Wolff, 2012; Wolff et al., 2012). The hypothesis arising from those observations is that circuits defining the ancestral mushroom body column had undergone an evolved transition to become subsumed into the mushroom body calyx, providing the prototypic morphology of a reptantian hemiellipsoid body (Wolff et al., 2012). A competing hypothesis would be that the mushroom body-like circuits in the hemiellipsoid body of Anomura represent convergent evolution.

The hemiellipsoid body of *C. clypeatus* is alone unable to provide further support for a mushroom body ancestry. However, molecular phylogenies (Wolfe et al., 2019) demonstrate the infraorder Anomura as a taxon-rich lineage. Coenobitidae belongs to a lineage of semiterrestrial anomurans that diverged within Paguroidea (hermit and king crabs) approximately 35 million years ago. Their early stages of development are marine, but they spend most of their lives on land, other than to mate. The older group Paguroidea, from which Coenobitidae derives, includes Paguridae, a family of entirely marine hermit crabs that might offer insights both into the evolution of the coenobitoid hemiellipsoid body as well as its neuroanatomical affinities to corresponding centers in Astacidea and Achelata, two infraorders of the other major branch of Reptantia for which there is neuroanatomical information (Sullivan & Beltz, 2004, 2005).

To investigate whether there are characters in Anomura that typify mushroom bodies, as defined in insects and stomatopods (Wolff et al., 2017), we here compare the hemiellipsoid bodies of the marine "hairy" hermit crab *Pagurus hirsutiusculus* (McLaughlin, Komai, Lemaitre, & Listyo, 2010) with the hemiellipsoid bodies of the crayfish *Procambarus clarkii* (Girard, 1852) and *Orconectes immunis*, species within the infraorder Astacidea. *P. clarkii* has been used for numerous studies of crustacean olfaction, which have focused on the electrophysiological properties of its hemiellipsoid body in the context of integrating olfactory coding with other sensory modalities (Mellon, 2000; McKinzie, Benton, Beltz & Mellon, 2004). This species has also been utilized for resolving the hemiellipsoid body's relationship to the reptantian olfactory pathways, from their origin in the deutocerebrum to their termination in the lateral protocerebrum (Sullivan & Beltz, 2001a).

Here, we describe the discovery of neuroanatomical arrangements that demonstrate that the *Pagurus* hemiellipsoid body possesses a chimeric morphology. Its composition suggests that circuitry typifying a columnar mushroom body lobe has been largely subsumed into a calyx-like neuropil. However, in *Pagurus* orthogonal networks like those of the *C. clypeatus* hemiellipsoid body supplies fibers to a columnar lobe corresponding morphologically to one of two types identified for the mushroom body of the caridean shrimp, *Lebbeus groenlandicus* (Sayre & Strausfeld, 2019). In *Pagurus*, the columnar lobe extends mediocaudally from its calycal origin assuming the same trajectory as observed for mushroom body columnar lobes in Stomatopoda (Wolff et al., 2017). Here, we provide data from Paguroidea showing that compared with distant outgroups Caridea and Stomatopoda, the ancestral mushroom body organization has been retained, whereas in Achelata and Astacidea it has not. In their astacid representatives *P. clarkii* and *O. immunis*, the ancestral columnar lobe typifying mushroom bodies has been entirely lost with a concomitant (and radical) reorganization of ancestral neural networks into two discrete but adjoining neuropils. The present results speak forcefully against the achelate and astacid hemiellipsoid bodies as representative of the cerebral ground pattern of Malacostraca, and instead speak

for the iconic mushroom body morphology being the ancestral ground pattern of Eumalacostraca. Hemiellipsoid bodies in reptantians other than certain Anomura are thus highly derived, having modified many attributes of their ancestral organization.

2 | MATERIALS AND METHODS

2.1 | Crustacean species

Hermit crabs belonging to the species *P. hirsutiusculus*, henceforth usually referred to simply by the genus *Pagurus*, were collected from designated sites on San Juan Island, WA, and maintained at the Friday Harbor Research Facilities (University of Washington; Friday Harbor, WA). Animals used for immunohistochemistry and Golgi impregnations were processed on site. Some animals used for silver staining were sent to the University of Arizona for processing. Hermit crabs were kept in marine tanks that approximated an intertidal environment with sand and pebble raised beds as well as seawater that approximated the salinity of ocean water at the time of capture. Crayfish species *P. clarkii* and *O. immunis* were purchased from Carolina Biological Supply Co. (Burlington, NC) and maintained in fresh water aquaria, also at the University of Arizona's Department of Neuroscience. Animals were fed a diet of blood worms and dehydrated shrimp and were kept on a 12-hr light/dark cycle.

2.2 | Golgi impregnations

Single Golgi impregnations were utilized to reveal the morphologies of individual or small groups of neurons. Double impregnations were adjusted to selectively impregnate substantial populations of neural assemblies. Animals were anesthetized by cooling. Their brains and neural tissue in the eyestalks were dissected out and desheathed in fixative containing 1 part 25% glutaraldehyde to 5 parts 2.5% potassium dichromate with 3% sucrose. Neural tissue was left to incubate in fixative for 2–4 days at room temperature in the dark. Following this, neural tissue was well rinsed in 2.5% potassium dichromate (without sucrose) and immersed overnight in a solution comprising 2.5% potassium dichromate and 0.01% osmium tetroxide. The next day, neural tissue was transferred quickly from the osmium solution into two changes of 0.75% silver nitrate, and then into a fresh solution of 0.75% silver nitrate where it was left in the dark for 24 hr. For sparse neuronal impregnation, tissue was then dehydrated and embedded. For impregnation of large numbers of neurons, often having similar morphologies, the osmium-dichromate and silver nitrate steps were repeated once more before dehydration and embedding.

Following single or double impregnation, neural tissue was dehydrated through an ascending ethanol series of 50, 70, and 90, and twice in 100%, each for 10 min. Neural tissue was transferred into propylene oxide for 15 min and then embedded in increasing concentrations of Durcupan embedding medium (Sigma Aldrich; Cat# 44610; St. Louis, MO) diluted in propylene oxide at ratios of 1:3, 1:1, and 3:1 over the course of at least 3 hr. Finally, tissue was transferred into 100% Durcupan, left overnight, and then polymerized in an oven at 60 °C for about 12–24 hr. Once polymerized and cooled, tissue sections were cut at 30–40 μm using a sliding microtome and mounted on slides using Permount mounting medium (Fisher Scientific; Cat# SP15-100; Hampton, NH).

2.3 | Antibodies

Visualization of arrangements that define hemiellipsoid bodies and mushroom bodies was achieved immunohistochemically using antibodies listed in Table 1. An antibody against DC0 that recognizes the catalytic subunit of protein kinase A in *D. melanogaster* (Skoulakis et al., 1993) is preferentially expressed in the columnar lobes of mushroom bodies across invertebrate phyla, including members of Lophotrochozoa (Wolff & Strausfeld, 2015). Western blot assays of DC0 antibodies used on cockroach, crab, centipede, scorpion, locust, remipede, and millipede neural tissue reveal a band around 40 kDa, indicating cross-phyletic specificity of this antibody (Stemme, Iliffe, & Bicker, 2016; Wolff & Strausfeld, 2015). Antibodies against synapsin (Klagges et al., 1996) and α-tubulin (Thazhath, Liu, & Gaertig, 2002) were used, often in conjunction with other primary antibodies, to identify dense synaptic regions and general cellular connectivity. Both antibodies likely recognize highly conserved epitope sites across Arthropoda and have been used previously in crustaceans (Andrew, Brown, & Strausfeld, 2012; Brauchle, Kiontke, MacMenamin, Fitch, & Piano, 2009; Harzsch, Anger, & Dawirs, 1997; Harzsch & Hansson, 2008; Sullivan, Benton, Sandeman, & Beltz, 2007).

Antibodies against serotonin (5HT), glutamic acid decarboxylase (GAD), and tyrosine hydroxylase (TH) were used in this study to describe neuronal organization and in distinguishing neuropil boundaries. 5HT is an antibody that has proven to be invaluable for neuroanatomical studies across Arthropoda (Antonsen & Paul, 2001; Harzsch & Hansson, 2008; Nässel, 1988). Previous studies have used 5HT as a comparative tool for neurophylogenetic analysis (Harzsch, 2004; Harzsch & Waloszeck, 2000). Antibodies against GAD and TH were used here to detect the enzymatic precursors of gamma-aminobutyric acid (GABA) and dopamine, respectively. These two antibodies do not require the use of alternative fixation methods, making them compatible with synapsin and α-tubulin labeling, while avoiding the need to use glutaraldehyde. Comparisons of anti-GAD and anti-TH immunolabeling with that of their respective derivatives have demonstrated that these antibodies, respectively, label putative GABAergic and dopaminergic neurons (Cournil, Helluy, & Beltz, 1994; Crisp, Klukas, Gilchrist, Nartey, & Mesce, 2001; Stemme et al., 2016; Stern, 2009).

2.4 | Immunohistochemistry

The methods described here are those used in two recent studies on the eumalacostracan brain (Sayre & Strausfeld, 2019; Wolff et al., 2017). To immunolabel crustacean neural tissue, animals were anesthetized to immobility using ice. Brains detached from nerve bundles leading to the eyestalks were first dissected free and the eyestalks were then removed. Both were immediately placed into ice-cold

TABLE 1 Primary antibodies used in this study

Antibody	Concentration	Host	Immunogen	Supplier; catalogue #; RRID
α-Tubulin	1:100	Mouse (monoclonal)	α-Tubulin derived from the pellicles of the protozoan *Tetrahymena*	DHSB; 12G10; AB_1157911
Synapsin (SYNORF1)	1:100	Mouse (monoclonal)	*Drosophila* glutathione S-transferase- fusion protein	DHSB; 3C11; AB_528479
Serotonin (5HT)	1:1000	Rabbit (polyclonal)	Serotonin coupled to bovine serum albumin with paraformaldehyde	ImmunoStar; 20080; AB_572263
Glutamic acid decarboxylase (GAD)	1:500	Rabbit (polyclonal)	C-terminal of both the 65- and 67-kDa isoforms of human GAD	Sigma Aldrich; G5163; AB_477019
Tyrosine hydroxylase (TH)	1:250	Mouse (monoclonal)	TH purified from rat PC12 cells	ImmunoStar; 22941; AB_572268
DC0	1:400	Rabbit (polyclonal)	Catalytic subunit of *Drosophila* protein kinase A	Generous gift from Dr. Daniel Kalderon

fixative containing 4% paraformaldehyde in 0.1 M phosphate-buffered saline (PBS) with 3% sucrose (pH 7.4). Eyestalk neural tissue was dissected out and desheathed, as was the brain. Both were left to fix overnight at 4 °C. The following day, neural tissue was rinsed twice in PBS and then transferred to an embedding medium consisting of 5% agarose and 7% gelatin. Tissue was left in this medium for 30 min to 1 hr at 60 °C and then cooled to room temperature in plastic molds. Once the medium had solidified, the tissue-containing gelatin blocks were removed from the molds and postfixed in 4% paraformaldehyde in PBS for 1 hr at 4 °C. Next, the blocks were rinsed twice in PBS and sectioned at 60 μm using a vibratome (Leica VT1000 S). Tissue sections were then washed twice over a 20-min interval in PBS containing 0.5% Triton-X (PBST). Tissue was subsequently blocked in PBST with 0.5% normal donkey serum (NDS; Jackson ImmunoResearch; RRID:AB_2337258) for 1 hr before primary antibody incubation. Primary antibodies were added to the tissue sections at the dilutions listed in Table 1, and the sections were left overnight on a rotator at room temperature.

The next morning, sections were rinsed in PBST six times over the course of 1 hr. Donkey anti-mouse Cy3 and donkey anti-rabbit Cy5 or Alexa 647 (Jackson ImmunoResearch; RRID: AB_2340813; RRID: AB_2340607; RRID: AB_2492288, respectively) IgG secondary antibodies were added to Eppendorf tubes at a concentration of 1:400 and spun for 12 min at 11,000 *g*. The top 900 μL of the secondary antibody solution was added to the tissue sections, which were then left to incubate overnight at room temperature on a rotator. For F-actin staining, tissue sections were left to incubate in a solution containing phalloidin conjugated to Alexa 488 (Thermo Fisher Scientific; RRID: AB_2315147) at a concentration of 1:40 in PBST for 2–3 days with constant gentle agitation following secondary antibody incubation.

To label cell bodies, tissue sections were then rinsed twice in 0.1 M Tris–HCl buffer (pH 7.4) and soaked for 1 hr in Tris–HCl buffer containing 1:2000 of the nuclear stain, Syto13 (ThermoFisher Scientific; Cat# S7575) on a rotator. Next, sections were rinsed six times in Tris–HCl over the course of 1 hr before being mounted on slides in a medium containing 25% Mowiol (Sigma Aldrich; Cat# 81381) and 25% glycerol in PBS. Slides were covered using #1.5 coverslips (Fisher Scientific; Cat# 12-544E). To verify secondary antibody specificity, primary antibodies were omitted resulting in complete abolishment of immunolabeling.

TH immunolabeling required a modified staining procedure with a shorter fixation time as well as antibody incubation in whole unsectioned tissue. Standard fixation times or sectioning the tissue prior to immunostaining resulted in poor or absent labeling as has been described previously (Cournil et al., 1994; Lange & Chan, 2008). For TH labeling, neural tissue was dissected and fixed in 4% paraformaldehyde in PBS containing 3% sucrose for 30–45 min. Following fixation, neural tissue was rinsed twice in PBS, and then twice in 0.5% PBST over the course of 40 min. Tissue was then transferred to blocking buffer containing 5% NDS in 1% PBST and left to soak for 3 hr. TH primary antibody was next added to the blocking buffer at a concentration of 1:250. To assist antibody permeation, whole tissues were microwave-treated for 2 cycles of 2 min on low power (~80 W) followed by 2 min no power under a constant vacuum. Tissue was subsequently left to incubate in primary antibody solution for 2–3 days and was microwave-treated each day.

After primary antibody incubation, tissue was washed with 0.5% PBST six times over the course of 2 hr and then transferred to a solution containing 1:250 Cy3 secondary antibody. Whole mounts were left in secondary antibody overnight on a gentle shaker before being sectioned and mounted as described above. In dual labeling experiments, sectioned tissue labeled with anti-TH was then stained with an additional primary and secondary antibody also as described above.

2.5 | Imaging

Confocal images were collected using a Zeiss Pascal 5 or LSM880 confocal microscope (Zeiss; Oberkochen, Germany). Image projections were made using FIJI (z project plugin; Schindelin et al., 2012). Brightness, contrast, and color intensity were adjusted using Adobe Photoshop CC (Adobe Systems; San Jose, CA), employing the camera raw filter plug-in for initial dehazing and intensity adjustment. Light microscopy images were obtained using a Leitz Orthoplan microscope equipped with PlanApochromat oil-immersion objectives (X40, X60, and X100). Series of step-focused image sections (0.5–1.0 μm increments) were stitched together and reconstructed using Helicon Focus (Helicon Soft; Kharkov, Ukraine) or employing the darkening function on Photoshop layering.

3 | TERMINOLOGY

The hemiellipsoid body of the crayfish *P. clarkii* comprises two discrete volumes—a rostral neuropil surmounting a second volume beneath. Ideally, to exclude any unintended bias in interpreting possible homologues, the preference would be to use already published terms to refer to these neuropils. However, an important study by Blaustein et al. (1988) demonstrates the difficulty in doing so. That study designated the upper of the two stacked neuropils of the *P. clarkii* hemiellipsoid body as "neuropil II" and the lower as "neuropil I." The same notations, however, are also used to denote two adjacent hemiellipsoid body neuropils in the spiny lobster *Panulirus argus* (Blaustein et al., 1988). Lack of an anatomical basis for homologizing neuropils "I" and "II" in these two reptantian lineages (Astacidea and Achelata) requires a renaming of these neuropils in one of the species. Mindful of the extensive work on the *Procambarus* olfactory system (Mellon, 2003; Mellon, 2016; Sullivan & Beltz, 2001a, 2001b) but because this article focuses on this species, we have renamed "neuropil II" as the "cupola" and "neuropil I" beneath it, the "torus". Our terminology for components of the *Pagurus* mushroom body reflects previous studies. Following the convention adopted *for L. groenlandicus* (Sayre & Strausfeld, 2019), the two calycal neuropils of *Pagurus* are termed calyx 1 and calyx 2 and their constituent layers numbered 1–3. Other nomenclature mainly follows that introduced by Blaustein et al. (1988) and by Sandeman and Scholtz (1995).

4 | RESULTS

4.1 | Comparison of anomuran and astacid brains

Although *P. hirsutiusculus* and *P. clarkii* are both reptantians, their brain organization differs markedly with regard to their deutocerebra (Figure 1). Whereas both species possess paired accessory lobes, the defining brain region of Reptantia (Sandeman, Scholtz, & Sandeman, 1993), these differ markedly in size. As already noted by Sandeman et al. (1993) from observations of marine and land hermit crabs (*Pagurus sinuatus* and *C. clypeatus*) and a study of the European hermit crab *P. bernhardus* (Krieger et al., 2012), the anomuran accessory lobe is minute compared with those typifying Astacidea and Achelata. In *P. hirsutiusculus*, the accessory lobe comprises some 60–80, approximately ball-shaped units, in contrast to the several thousand that comprise the accessory lobe of *P. clarkii*. In *Pagurus*, although the lobe receives inputs from the adjacent olfactory lobe, its subunits do not clearly define a distinct outer layer and inner core like that described for the crayfish (Sullivan & Beltz, 2005), nor is the lobe obviously connected to its contralateral counterpart as occurs in the crayfish. The size of the anomuran accessory lobe precludes it from contributing many axons to the olfactory globular tract (OGT), the primary route taken by olfactory relays from the deutocerebrum to the lateral protocerebrum. In *P. clarkii* and members of Achelata, such as the spiny lobster *P. argus*, the accessory lobe receives its main afferent supply from the olfactory lobes with afferents into the accessory lobe segregating to distinct concentric zonations (Sandeman & Luff, 1973; Schmidt & Ache, 1997). In Achelata, as in Astacidea, the accessory lobes are connected to their contralateral counterparts by a massive horizontal tract (Sandeman & Luff, 1973), and they provide the dominant olfactory input to the lateral protocerebrum (Sullivan & Beltz, 2001a). As shown in the comparative overview of Figure 1, these distinctions contribute to the defining differences of anomuran and astacid deutocerebral morphologies, as shown by Sandeman et al. (1993). The organization of the olfactory lobes further distinguishes Anomura from Astacidea. Anomuran olfactory lobes are composed of characteristically spindle-shaped subunits (classically referred to as glomeruli), whereas in Astacidea, each "glomerulus" has a distinctive broader, shorter shape, thus assuming more of a wedge-like geometry. The glomeruli in anomuran olfactory lobes far outnumber those of Astacidea irrespective of the relative size of their brains (Figure 1).

Whether these deutocerebral distinctions are linked to differences between the lateral protocerebra of Anomura and Astacidea is not known. Here, attention is directed to the most pronounced features of the lateral protocerebra, namely centers that are the primary recipients of relays from the olfactory centers in the deutocerebrum (Figure 1) and which are associated with a population of thousands of minute globuli cell bodies that provide intrinsic neurons (Figure 1). If the center demonstrates traits that define a columnar mushroom body, then we refer to the center as a mushroom body. If the center shows no evidence of a columnar lobe, but nevertheless comprises intrinsic neurons derived from clustered globuli cells, we refer to it as a hemiellipsoid body. The primary consideration of this article—that neuroanatomical observations support the view that the hemiellipsoid bodies are mushroom body homologues—will be considered in the Discussion after the following sections compare and contrast these centers.

4.2 | The double calyx of *Pagurus*

Selective affinity to anti-DC0 (Figure 2a–c) reveals in the lateral protocerebrum of *Pagurus* a prominent structure (Figure 1c) comprising two adjacent calyces. Within each calyx, axon-like processes collect to form a bundle, which divides each calyx into three layers with

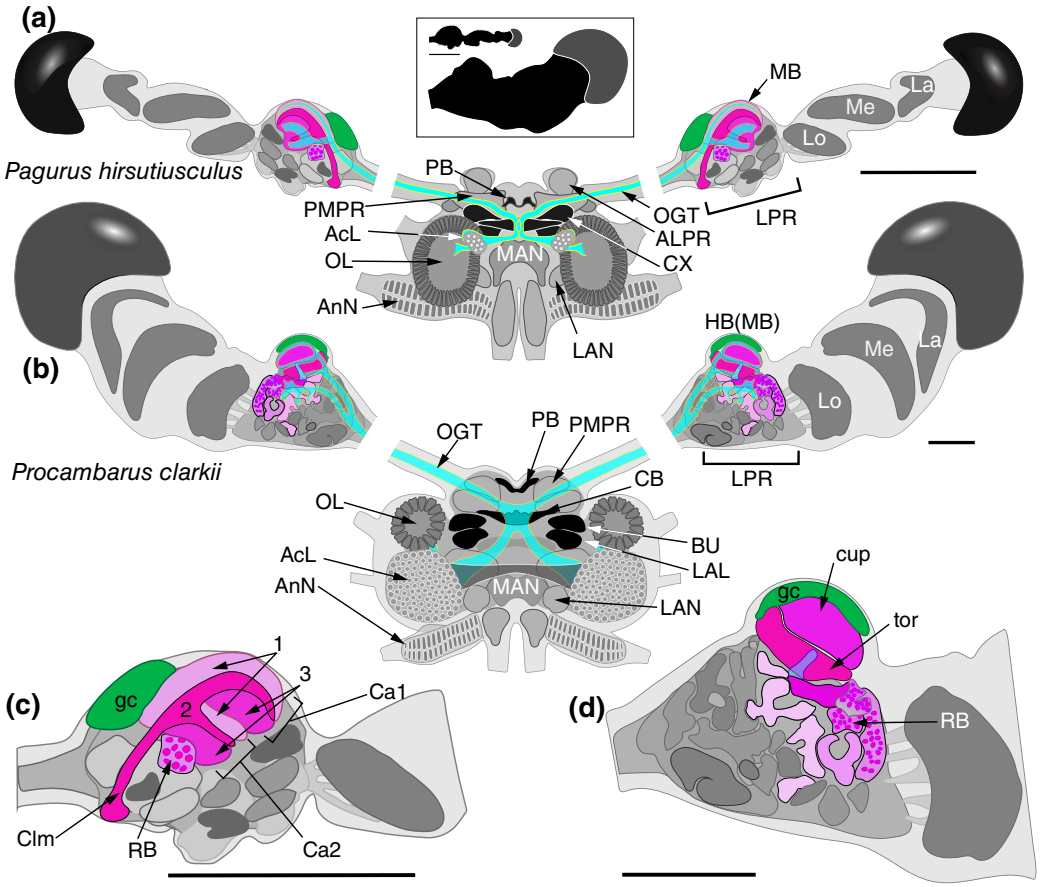

FIGURE 1 Overview of the brains of the marine hermit crab *P. hirsutiusculus* and the crayfish *P. clarkii*. Center top inset demonstrates the relative size of their eyestalk neuropils surmounted distally by the compound eye. (a) Schematic of *Pagurus* brain and major neuropils. (b) Schematic of *Procambarus* brain and major neuropils. Abbreviations: AcL, accessory lobe; ALPR, anterior lateral protocerebrum; AnN, antenna 2 neuropil; BU, lateral bulb of the central complex; CB, central body; CX, central complex (central body, lateral bulb); LAL, lateral accessory lobe; LAN, lateral antennular lobe neuropil; La, lamina; Lo, lobula; LPR, lateral protocerebrum; MAN, median antenna 1 neuropil; MB, mushroom body; HB (MB) hemiellipsoid body-mushroom body derivative; Me, medulla; OL, olfactory lobe; OGT, olfactory globular tract; PMPR, posterior median protocerebral neuropils; PB, protocerebral bridge. (c) Schematic of the right *Pagurus* lateral protocerebrum. Abbreviations: Ca1, Ca2, the paired and adjoining calyces; 1, 2, 3, outer, middle, and inner calycal layers; Clm, mushroom body columnar lobe; gc, globuli cell body layer; RB, reniform body. (d) Schematic of the right *Procambarus* lateral protocerebrum. Abbreviations: cup, hemiellipsoid body cupola; gc, globuli cell body layer; tor, hemiellipsoid body torus; RB, reniform body. Neuropils that show strong to weak DC0 affinity are indicated by graded intensities of magenta. All scale bars = 500 μm

the bundle as layer 2 interposed between layers 1 and 3. Layers 2 from each calyx converge proximally and thereafter continue proximally as a columnar lobe (Figure 2c,d). The layered architecture is similar to the organization described from the land hermit crab *C. clypeatus*, where the cap neuropil corresponds to the *Pagurus* layer 1 and where extensions of its intrinsic neurons beneath its second layer provide many stratified orthogonal arrangements nested within its domed volume (Wolff et al., 2012).

In *Pagurus*, a prominent cluster of small basophilic cell bodies (globuli cells) is situated rostrally above the lateral protocerebrum and extends distally over approximately one-fifth of the calyces. The globuli cells provide extremely thin cell body fibers that give rise to the intrinsic neuron arbors, the bistratified dendrites of which extend into layers 1 and 3 (Figure 3). The arrangement of two immediately adjacent calyces is reminiscent of organization in the caridean species *L. groenlandicus*, where in each lateral protocerebrum, there are also two calyces, both organized into three distinct layers. But in *Lebbeus*, the calyces are entirely separate (Sayre & Strausfeld, 2019).

The double calyx of *Pagurus* supplies a single columnar lobe, which extends across the lateral protocerebrum to terminate mediocaudally (Figures 1 and 2). Many hundreds of axon-like prolongations from intrinsic neurons from both layers 2 converge at the adjoining proximal margins of the two calyces and coalesce to proceed further as a single lobe (Figure 2c,d). Just before they enter the columnar lobe, the intrinsic neuron fibers are associated with a dense arrangement of local interconnections (synaptic zone in Figure 3). Because each calyx contributes intrinsic neuron fibers, we interpret the lobe as a fusion of two lobes, which may be reflected by the four tubercle-like swellings at the lobe's terminus. The swellings correspond to those observed terminating the larger of the two columnar lobes of the mushroom body of *L. groenlandicus* (Clm2, in Sayre & Strausfeld, 2019), and typify the morphologies of columnar neurons in Zygentoma and Ephemeroptera, both

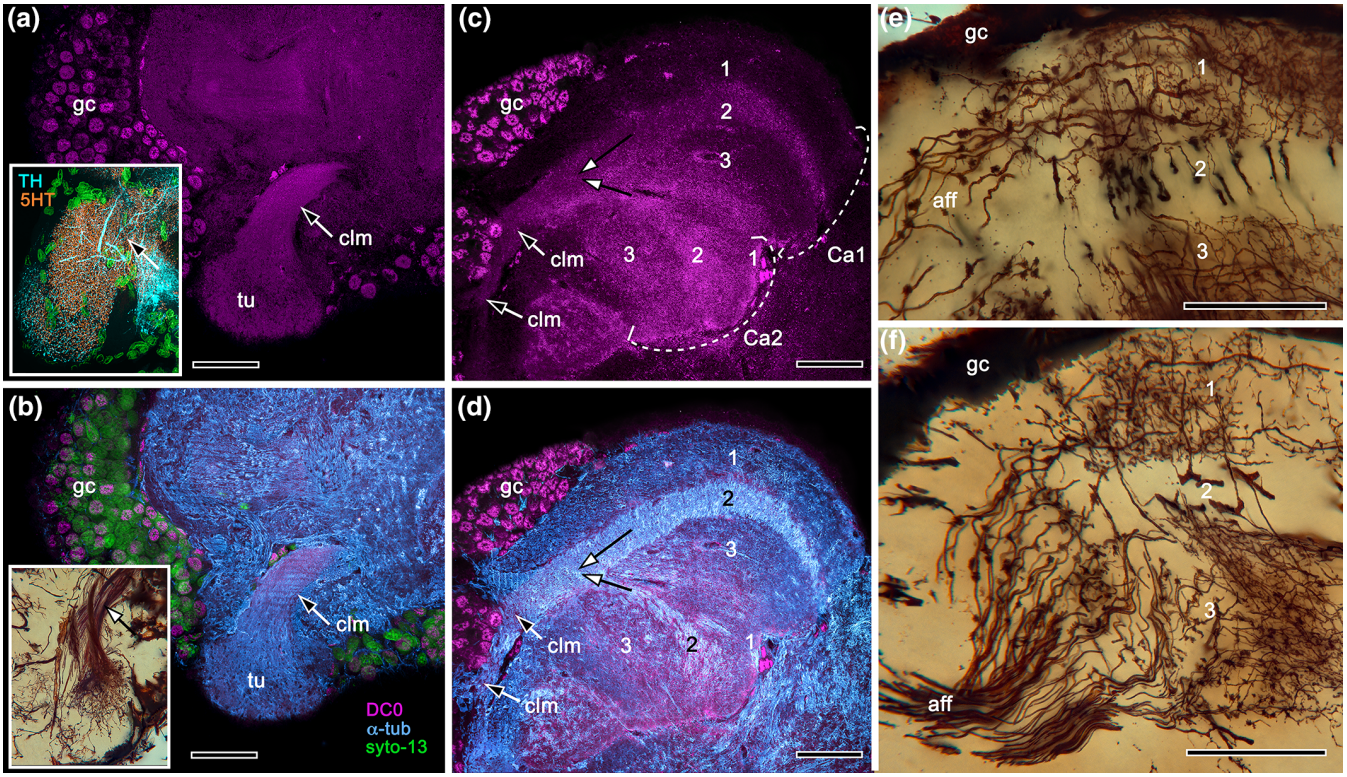

FIGURE 2 Columnar lobe and calyces of the *Pagurus* mushroom body. (a, b) confocal scans showing higher anti-DC0 immunoreactivity in globuli cell bodies (gc) and in the mushroom body's columnar lobe (clm) and terminal comprising a cluster of tubercles (tu) into which the axon-like fibers of intrinsic neurons branch (inset in b). These fibers are intersected by aminergic arborizations of neurons leading off into the lateral protocerebrum (inset in a). (c, d) Confocal scans showing distribution of anti-DC0 immunoreactivity in calyx 1 and calyx 2 (Ca1, Ca2) each segmented into three layers, two of which (2,3) show elevated anti-DC0 immunoreactivity. Due to the curvature of the neuropil, the calyx 1 layers are seen from the lateral aspect, whereas those of calyx 2 are viewed obliquely from above. Converging arrows indicate the passage of intrinsic neuron fibers merging at this point to extend further into the columnar lobe (clm). Counterstaining with the nuclear stain syto13 (b) reveals that only some globuli cells (gc) are anti-DC0 immunoreactive, indicating that only a subpopulation of intrinsic cells may be directly involved in memory acquisition. (e, f) Afferent terminals (aff) from the olfactory globular tract extend into layers 1 and 3, where their endings provide numerous bead-like presynaptic specializations along their lengths. Scale bars a–f = 50 μm

basal insects (Farris, 2005; Strausfeld, Sinakevitch, Brown, & Farris, 2009). Two of the four columns of the stomatopod mushroom body have comparable trajectories (Wolff et al., 2017). As occurs in those crustacean species, in *Pagurus* intrinsic neuron processes branching in the tubercles are intersected by anti-TH and anti-5HT immunoreactive arborizations (inset of Figure 2a).

The two calyces are supplied by thousands of terminals of relay neurons from the OGT (Figure 1a). The OGT expands at the proximal margin of the double calyx to provide bundles of terminals extending into layers 1 and 3 of each calyx (Figure 2e,f). The terminals project along the full extent of their respective layers, where they provide numerous varicose specializations (Figure 2e,f). The OGT also provides a tributary that extends into lateral protocerebral neuropils beneath and distal to the calyces, as occurs in the land hermit crab *C. clypeatus*.

4.3 | Intrinsic neurons of the anomuran calyx

As for the stomatopod and coenobitoid mushroom bodies, the standard double-impregnation Golgi method used on *Pagurus* results in spectacular mass impregnation of intrinsic neurons. Figure 3 summarizes the disposition of the adjoining calyces and their relationship with the columnar lobe and globuli cell bodies. Figures 4 and 5 show crucial aspects of neuronal arrangements in the calyx, each example referring to a specific part of the calyx's layered organization. Although both calyces have identically organized layers, the connection of intrinsic neurons to their globuli cell bodies is demonstrable only for the most proximal part of the calyx (Figure 4b). This is because the cluster of globuli cells is restricted to near the proximal margin of the lateral protocerebrum rather than extending above the entire calyx, as it does in *C. clypeatus* and in mantis shrimps. Thus, that part of layer 2 belonging to both calyces situated immediately beneath the globuli cell cluster is much expanded as it has to accommodate not only out-going intrinsic neuron axons to the columnar lobe but also the cell body fibers of all the calyx intrinsic neurons. These cell body fibers have to extend from the originating globuli cells to their corresponding neuronal arborizations, which can be hundreds of micrometers distant.

As shown by labeling the calyx's fibrous architecture with antibodies against α-tubulin (Figure 4a), both layers 2 eventually taper off

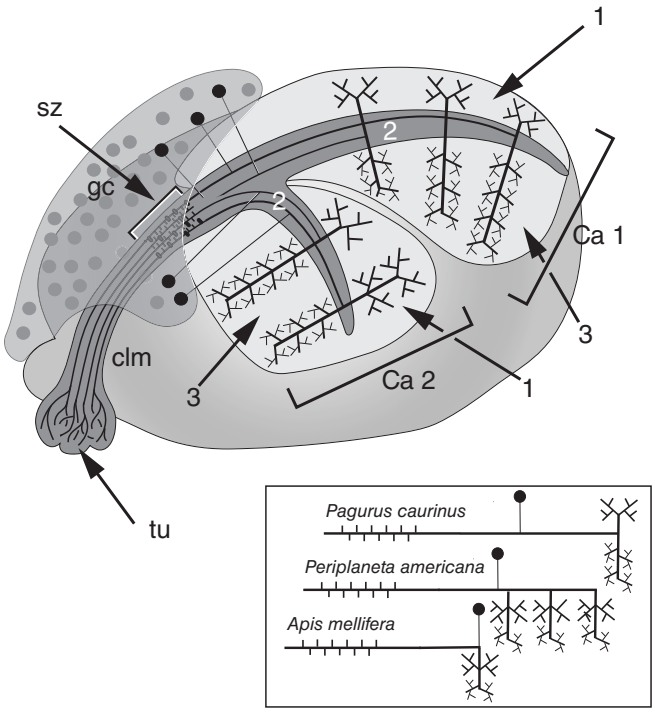

FIGURE 3 Schematic of the right *Pagurus* mushroom body. Globuli cells (gc) providing intrinsic neurons are clustered over the proximal flank of the lateral protocerebrum and underlying calyces. These are indicated as Ca1 and Ca2, and their layers as 1–3, layer 2 providing axon-like processes from the calyces into the columnar lobe (clm), which terminates as a tubercular bulb (tu). A small zone of interacting processes, the synaptic zone (sz), is located at the lobe's origin. The basic morphology of intrinsic neurons corresponds to those in the insect mushroom body (inset), where they possess several dendritic trees or a single stratified dendritic tree

as the number of intrinsic neurons diminishes toward the calyx's perimeter (Figure 4c).

In insects and stomatopods, different classes of intrinsic neurons, referred to as Kenyon cells in insects, are categorized on the basis of their morphological attributes, such as whether they possess robust processes and dendritic trees, whether these branch densely or are sparse, and what kinds of specializations decorate them (Strausfeld, 2002). The *P. hirsutiusculus* calyx appears to have at least four morphological types of intrinsic neurons categorized according to their fiber diameters, dendritic morphologies, varicosities, and spines indicating likely synaptic sites, and their participation in diffuse or in highly structured networks. The former type, denoted by its extremely slender processes, is particularly susceptible to mass impregnation revealing its contribution to a dense stratum of slender branches in layer 3 that together show no evidence of orthogonal circuitry (Figure 4d). This contrasts with systems of intrinsic neurons that show precise parallel alignment across the calyx's layer 3 (Figure 4g,h). Variations in intrinsic neuron morphology are also revealed in layer 2, where the axon-like processes of intrinsic neurons destined for the columnar lobe interweave with the main axial processes of intrinsic neurons that cross layer 2 to link their arborizations in layers 1 and 3 (Figure 4e). Whereas the largest axons extending the length of layer 2 can range from 3 to 4 μm in diameter (Figure 5b–d), some of those crossing layer 2 have diameters of 0.5 μm or less. These slender processes are either recurrent extensions of large-diameter neurons (Figure 5b) or are indicative of small-diameter intrinsic cells, such as those providing diffuse arrangements shown in Figure 4d, or in Figure 4f where neurons that cross layer 2 demonstrate a wide range of fiber diameters.

A characteristic feature of the hemiellipsoid body of *C. clypeatus* is the presence of layered orthogonal networks that, together, provide evidence of connections typifying the lobes of the insect mushroom body (Brown & Wolff, 2012). A comparable arrangement is resolved in *Pagurus* where parallel ensembles of intrinsic neurons extending from calycal layers 1 to layer 3 are intersected at right angles by other parallel systems, the two sets of neurons providing an orthogonal circuitry, as in *Coenobita* (Figure 4g,h).

These deeper systems of orthogonal circuits in layer 3 are distinct from those observed in layer 1. There, a distinct system of rectilinear arrangements consists of ensembles of parallel fibers that originate as collaterals from a species of slender intrinsic neuron that provides dendritic processes to layers 1 and 3 (Figure 5f). These collaterals are richly decorated with synaptic specializations that spatially coincide with the spacing of presynaptic swellings belonging to incoming relays from the OGT. Labeling this layer with phalloidin-Alexa 488 and antibodies raised against synapsin resolves a regular striate organization of synaptic complexes (compare Figure 5e,f). These are suggestive of, but more elaborate than, synaptic complexes between afferents and Kenyon cell dendrites demonstrated in the honey bee (Stieb, Muenz, Wehner, & Rössler, 2010), or in the outer calyx of the stomatopod mushroom body (Wolff et al., 2017).

4.4 | The anomuran columnar lobe

Golgi impregnations and labeling with anti-α-tubulin show that the calyx's layer 2 is widest immediately before the origin of the columnar lobe. The lobe itself is narrower than layer 2, which is itself broader than it is deep. Golgi impregnations of the origin of the columnar lobe show that fibers entering it become abruptly narrower. The smallest of these fibers provide a synaptic zone within the column denoted by their spines and varicosities (Figure 5g). From that point, the constituent fibers of the lobe are smooth and undecorated until they reach the tubercles where they branch extensively and are decorated with bead-like presynaptic specializations (Figure 2b, inset).

4.5 | The cambarid hemiellipsoid body

The following descriptions defer to crucial earlier observations by Sullivan & Beltz (2001a,b; 2004) that identified the origin and distribution of afferent terminals from the deutocerebrum's olfactory and accessory lobes, demonstrating their segregation into the lateral protocerebrum. In the following, we retain the name "hemiellipsoid body" for the center into which these terminals mainly distribute. This nomenclature originated from Bellonci's studies in 1882. However, as proposed even then by Bellonci, and deliberated in the discussion here, numerous lines of

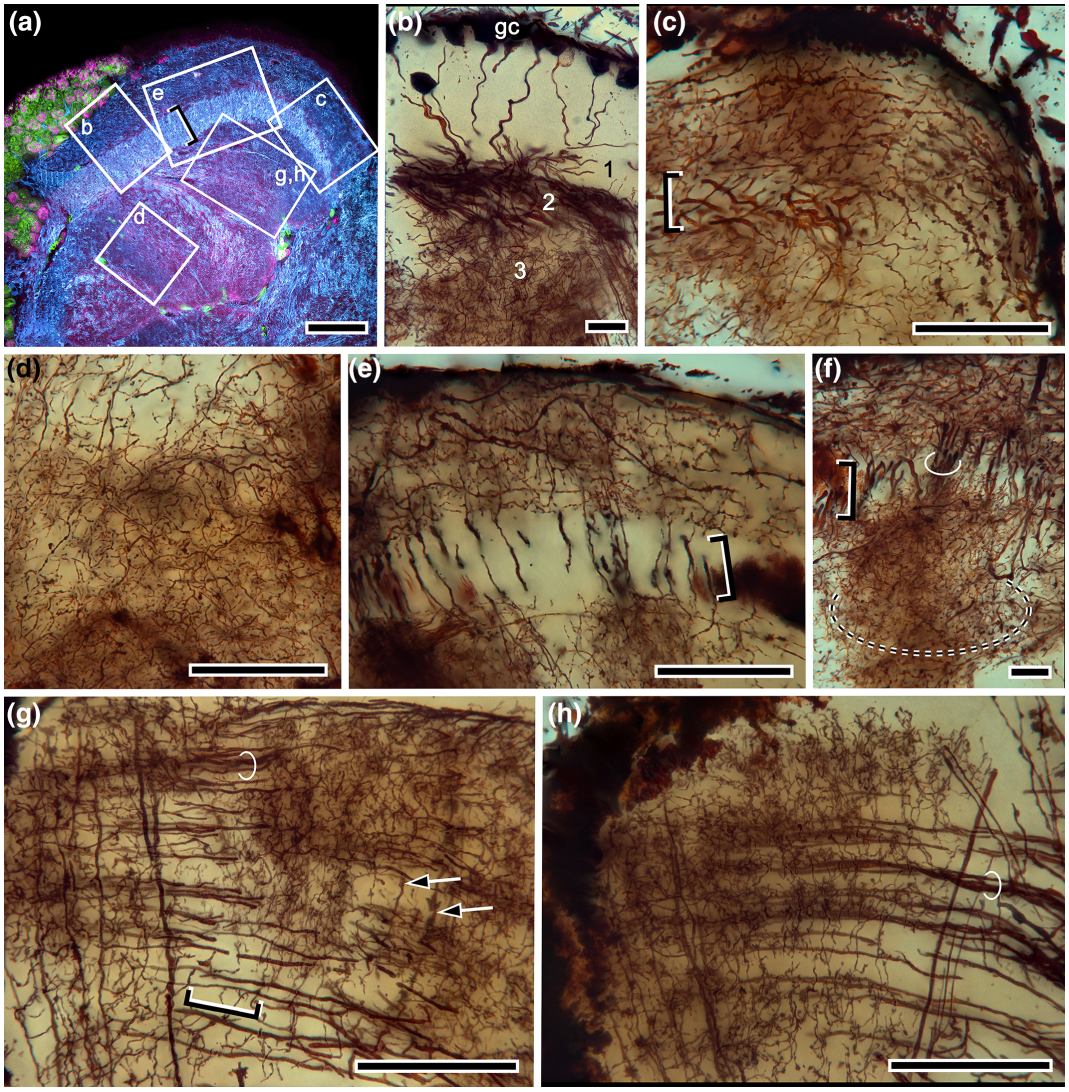

FIGURE 4 Neuronal organization of intrinsic neurons in the *Pagurus* calyces. (a) The best fit locations of areas showing the neurons in panels b–h. (b) Golgi-impregnated globuli cells shown with their cell body fibers extending into layer 2. (c) Terminal fibers, originating from the antennal lobe via the OGT, are shown occupying the whole depth of layer 1 even up to where layer 2 tapers distally. Layer 2 is indicated in this and other panels by the bracket. (d) System of diffuse local interneuron processes extending across a broad area of layer 3. (e) Prominent OGT terminals, recognizable by their swollen presynaptic specializations, branch among finer varicose processes belonging to a class of intrinsic neurons that extend across layer 2 to extend deep into layer 3. (f) That there are several types of intrinsic neurons is suggested by a bundle (circled) of connecting processes crossing between layers 1 and 3 to provide in the latter a substantial and dense volume (dashed line) of presynaptic (bead-like) and postsynaptic (spine-like) specializations indicative of elaborate circuitry in layer 3. (g) Oblique top-down view of layers 1–3 showing rectilinear arrangement in layer 1 (on the right) attributable, in part, to the passage of afferent processes from the OGT (arrowed), whereas in layer 3, two classes of intrinsic neurons are arranged orthogonally in a manner first identified in the hemiellipsoid body of *C. clypeatus* (Wolff et al., 2012). (h) Bundles (ringed) of parallel ranks of intrinsic neurons in layer 3, the axon-like processes of which extend into layer 2 and then to the columnar lobe. Scale bars = a, 50 μm; b, f, = 20 μm; c, d, e, = 50 μm; g, h, = 50 μm

evidence conclude that the hemiellipsoid body is the homologue of, and thus derived from, the ancestral columnar mushroom body.

4.6 | Organization and divisions of the cambarid hemiellipsoid body

The *Procambarus* and *Orconectes* hemiellipsoid bodies are virtually indistinguishable. Both of their hemiellipsoid bodies consist of two neuropils, one surmounting the other. The uppermost is a dome-like neuropil that surmounts a broader one beneath that is shaped like a torus. Both of these neuropils have historically been referred to as two neuropils of the unitary hemiellipsoid body, but they appear to be discrete centers (see the Discussion section). They are situated quite rostrally about half way between the proximal border of the lateral protocerebrum and the optic lobe's medulla (Figure 6a,b,d,e).

Labeling tissue to resolve its fibrous composition or synaptic aggregations using phalloidin, or anti-α-tubulin, in conjunction with anti-synapsin resolves the border delineating the two neuropils.

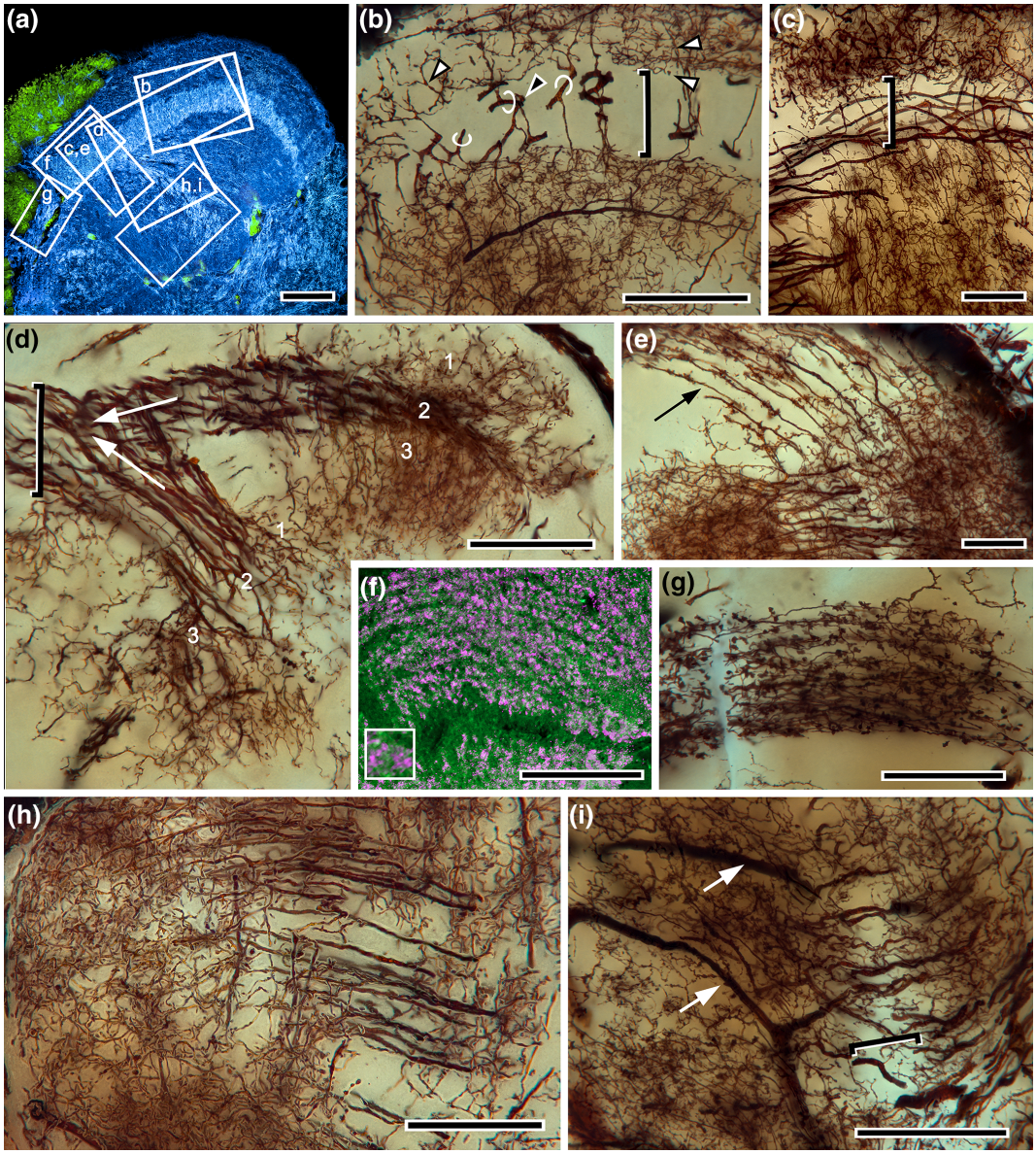

FIGURE 5 Neuronal organization of intrinsic neurons in the *Pagurus* calyces. (a) The best fit locations of panels b–i. (b) Cross section of layer 2 (bracketed) cutting perpendicular to the intrinsic cell axons showing portions of their fibers (circled), en route to the columnar lobe, that provide recurrent collaterals into layer 1 (black arrowhead). Note that in this layer there are elaborate systems of local connections (at and between white arrowheads) suggesting considerable synaptic complexity. (c) Intrinsic neuron fibers extending through layer 2 toward their exit point into the columnar lobe. (d) Composite stitched images of intrinsic neurons in Ca1 and Ca2 with dendritic arbors in layers 1, 3 and axon-like fibers in layers 2. Converging arrows indicate where layers 2 of each calyx merge to provide processes to the columnar lobe at the proximal margin of the calyces. (e) Systems of parallel collaterals (arrow) extending from another class of intrinsic neurons within layer 1's incoming system of terminals from the olfactory globular tract. (f) Serial synaptic aggregates within layer 1 demonstrated by immunolabeling with antisynapsin and phalloidin-Alexa 488. One synaptic aggregate is enlarged in the 4 μm x 4 μm inset, lower left. (g) Parallel fibers and synaptic plexus at the origin of the columnar lobe at the proximal margin of layer 2. (h) The parallel fiber motif is revealed by the majority of intrinsic neuron types (here in calyx 2), again suggesting its identity as a circuit typifying a columnar lobe but here subsumed into the calyx. (i) Major dendritic branches (arrowed) of efferent neurons that extend from layer 3 reveal an organization corresponding to organization of efferent neurons in the domed reptantian hemiellipsoid body. Scale = a,b, 25 μm; c, 25 μm; d–I, 50 μm

Antibodies raised against GAD show the same discrete border. As explained in the Terminology section of Materials and Methods, we call the upper neuropil the cupola (cup) and the lower one the torus (tor; Figure 6a–c). These correspond, respectively, to the original notations "neuropils II and I" employed by Sullivan and Beltz (2001a).

Anti-DC0 affinity to neural tissue is generally restricted to a mushroom body's columnar lobes. The exception is the reniform body, which in decapod crustaceans is an accessory visual center that has not yet been identified in Hexapoda. The reniform body shows selective affinity to DC0 in stomatopods and the caridean *L. groenlandicus*

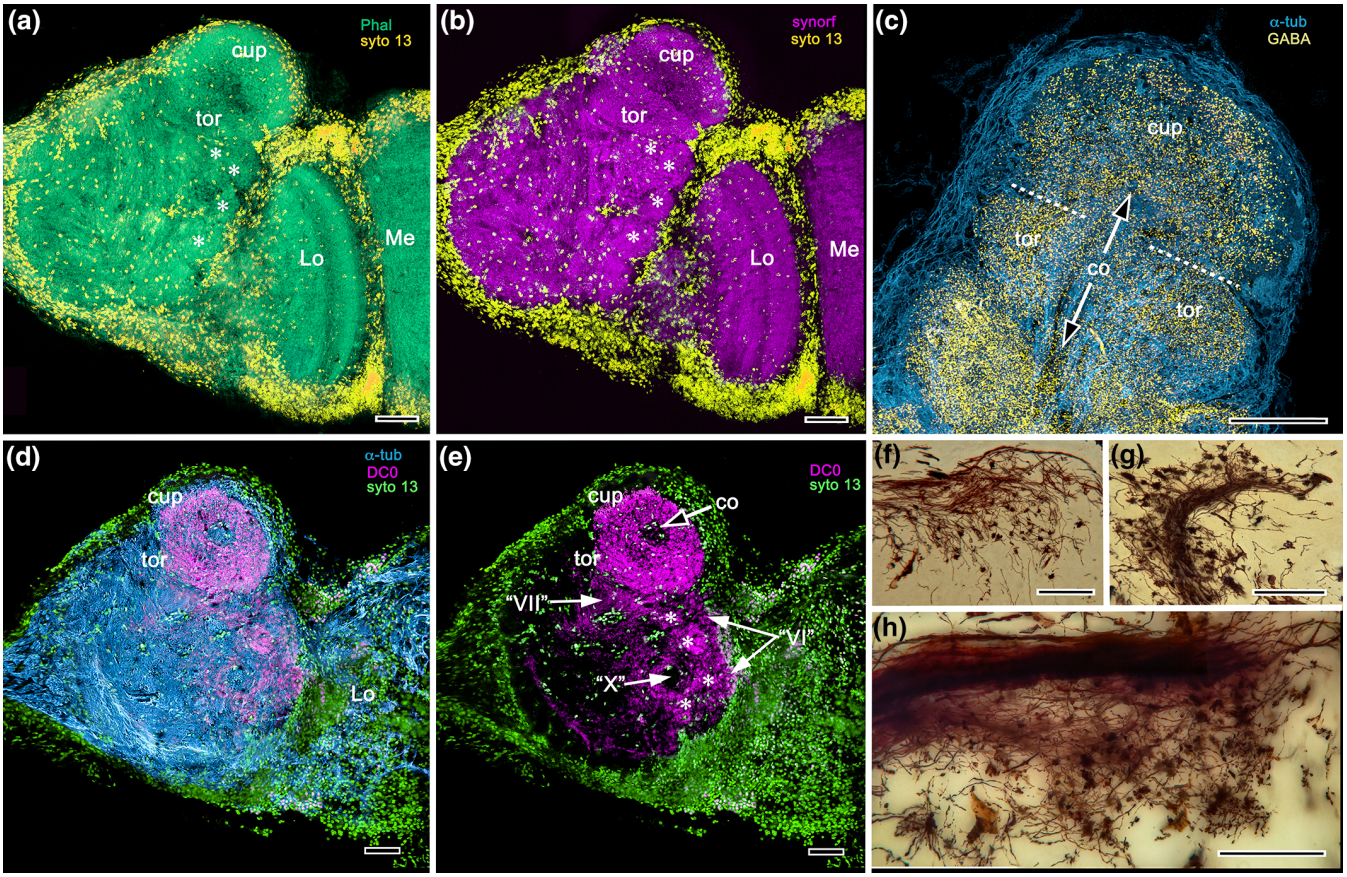

FIGURE 6 Overview of the *Procambarus* hemiellipsoid body and associated anti-DC0 immunoreactivity. Phalloidin-stained (a) and antisynapsin labeled (b) lateral protocerebrum demonstrating the characteristic rostral location of the hemiellipsoid body and its fairly distal location in the lateral protocerebrum. The cupola (cup) and torus (tor) are distinct, with the central channel (co, core) in the torus visible. Several well-defined neuropil volumes caudal to the hemiellipsoid body (asterisks) correspond to volumes identified by Blaustein et al. (1988) as being regions of very high synaptic density. (c) Anti-GAD immunoreactivity in the hemiellipsoid body demonstrates the clear distinction of its two neuropils (indicated by dotted line) and the central core of the torus reaching into the overlying cupola. (d, e) Anti-DC0 immunoreactivity selectively reveals the hemiellipsoid body and discrete neuropil beneath it, among which Area VII receives a major input from the olfactory lobes (Sullivan & Beltz, 2001a). "VII" and its adjacent volumes comprise large spheroidal patches of synaptic neuropil, corresponding to reniform body features identified in Stomatopoda (Wolff et al., 2017). (f) OGT terminals entering the rostral surface of the cupola. (g) OGT terminals ascending through the center of the torus and extending across its neuropil. (h) OGT terminals extending through Area VII beneath the hemiellipsoid body. Scale bars = a, b, d, e, 100 μm; c, f–h, 50 μm

(Sayre & Strausfeld, 2019; Wolff et al., 2017) and is resolved in the crayfish lateral protocerebrum. Although anti-DC0 appears to be a reliable marker for centers that phenotypically correspond to the columnar lobes of mushroom bodies, its affinity to hemiellipsoid body neuropils in *P. clarkii* and in *O. immunis* is somewhat different. Some specimens show intense labeling by anti-DC0 of the cupola and torus and, in addition, labeling in four discrete neuropils caudal and distal to these (in addition to the reniform body). These neuropils were originally identified by Blaustein et al. (1988) in silver-stained material and called neuropils "IV, V, VIII, and X". Of these all but neuropil "X" are to various degrees receptive to anti-DC0 (Figure 6d,e). In certain specimens, additional neuropils adjacent to those listed above show low affinity to anti-DC0 (Figure 1d). Further, several of these neuropils can be labeled with the DC0 antiserum even when, in some specimens, the hemiellipsoid body's torus is labeled but its cupola is not, as in Figure 8b. These variable expressions of DC0 will be further considered in the Discussion section.

4.7 | Neuronal organization in the cambarid hemiellipsoid body

An earlier study (McKinzie, Benton, Beltz, & Mellon, 2003) described neurons having extensive branching in either the cupola or torus of the hemiellipsoid body and sending axons into defined volumes of the ventrolateral protocerebrum. These efferent neurons will be discussed later as they provide important information regarding the functionality of these neuropils and the possible correspondence of these outputs with mushroom body efferents. Here, referring to Figures 6–8, we consider the neural organization exclusively within the cupola and the torus.

Compared with an insect or caridean mushroom body, a hemiellipsoid body has a relatively sparse globuli cell population resident above and lateral to its two neuropils (Figure 6d,e). As Sullivan and Beltz (2001a) demonstrated by lipophilic dye tracing, the outer and inner hemiellipsoid body layers receive different contributions of

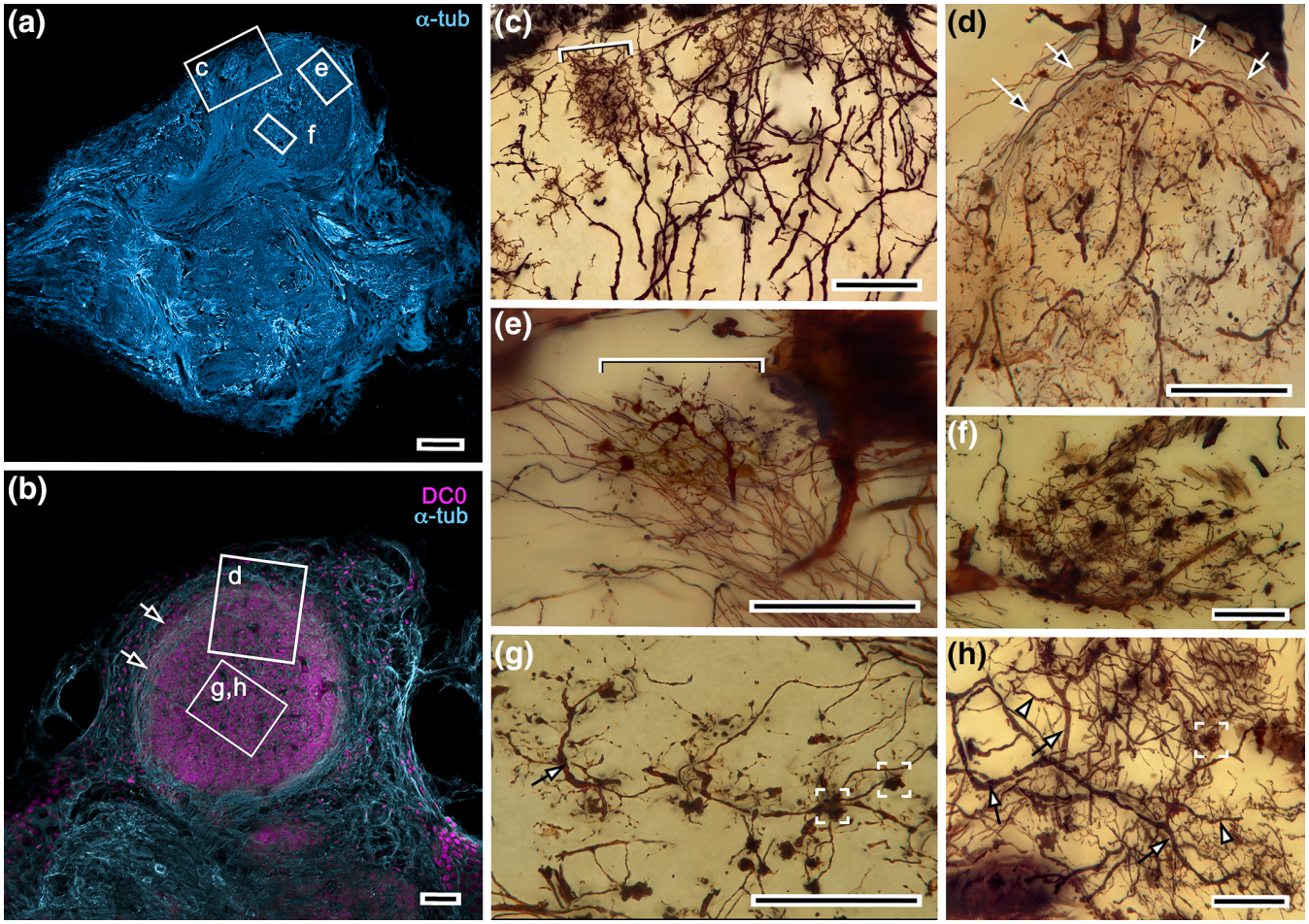

FIGURE 7 Neuronal organization in the crayfish hemiellipsoid body. (a) the best-fit locations of neurons in panels c, e, and f. (b) Oblique top-down view of the cupola of *O. immunis* showing elevated immunoreactivity to anti-DC0, indicating locations of neurons in panels d, g, and h. (c) Intrinsic neurons of the cupola showing their narrow bottlebrush-like dendritic trees just beneath the perimeter of the neuropil. The bracket indicates corresponding width of the enlarged tree in panel e. (d) Section across the cupola showing the projection of OGT axon terminals along its perimeter (arrows) and beaded collaterals in its deeper levels. (e) Converging OGT terminals onto the dendritic tree of an intrinsic neuron. (f) Collaterals extending among OGT terminals immediately beneath the cupola, at their exit from the torus's central core. (g) Local interneuron (arrow) extending across cupola neuropil showing a system of extremely slender collaterals some visited by one or several converging OGT terminals (boxed). This system contrasts with extensive large (arrows) and small diameter (arrowheads) local neurons in the torus (h). Scale bars = a, b, 100 μm; c–e, g, 50 μm; h, f, 20 μm

relays from the ipsi- and contralateral olfactory and accessory lobes. Terminal axons from the OGT enter the hemiellipsoid body at several locations, with fibers segregating to enter the cupola or torus. Axons to the cupola comprise a massive tract, the processes of which circle its perimeter before entering the layer's synaptic neuropil (Figures 6f and 7b). Axons to the torus extend to its lower margin and then distribute into the neuropil through its central core. There is also a massive input from the OGT to neuropils beneath the torus (Figure 6h), which distributes to a large volume of the neuropil designated "VII" by Blaustein et al. (1988). Terminals also reach into the volumes indicated by the upper two asterisks in Figure 6e and the outlined domain in Figure 8a, which features an exceptionally rich synaptic density (see Sullivan & Beltz, 2004).

The marginal neuropil of the cupola contains the serried dendritic trees of intrinsic neurons (Figure 7c), the axons of which extend deeper into the cupola where they provide terminal processes. The dendritic trees, which receive numerous dark swollen presynaptic boutons of OGT terminals, are equipped with spine-like specializations indicative of postsynaptic sites (Figure 7e). The trees are also associated with another system of dense arborizations composed of numerous fine branches that appear to be exclusively varicose, suggesting an extensive system of intermediary local interneurons associated between the dendrites of intrinsic neurons and terminals from the OGT converging onto them (Figure 8j,k).

Local circuits within the cupola include tangentially directed local interneuron processes that provide clusters of delicately branching collaterals extending to the terminal boutons of the OGT afferents (Figure 7g). These neural arrangements of the hemiellipsoid body's cupola are distinct from those in the torus where local circuits include both large- and small-diameter processes and extensive systems of branches (Figure 7h). For example, the core of the torus, through which OGT axons enter, reveals a system of interconnecting

processes among OGT terminals (Figure 7f). As shown in the synapsin-actin labeled inset of Figure 8a, the synaptic aggregates in the cupola are distinct from those of the torus and stratified into two levels. Golgi impregnations of the torus demonstrate axons from the OGT also entering it laterally and distributing in an approximate circle among a system of tangentially directed wide-diameter processes (Figure 8c). As the Golgi method selectively impregnates only a tiny proportion of any neuronal population, it is likely that such tangential systems are numerous. Compared with dendritic trees of intrinsic neurons in the cupola, those in the torus are broader, extending across its neuropils, where individual afferent boutons appose their dendrites (Figure 8d).

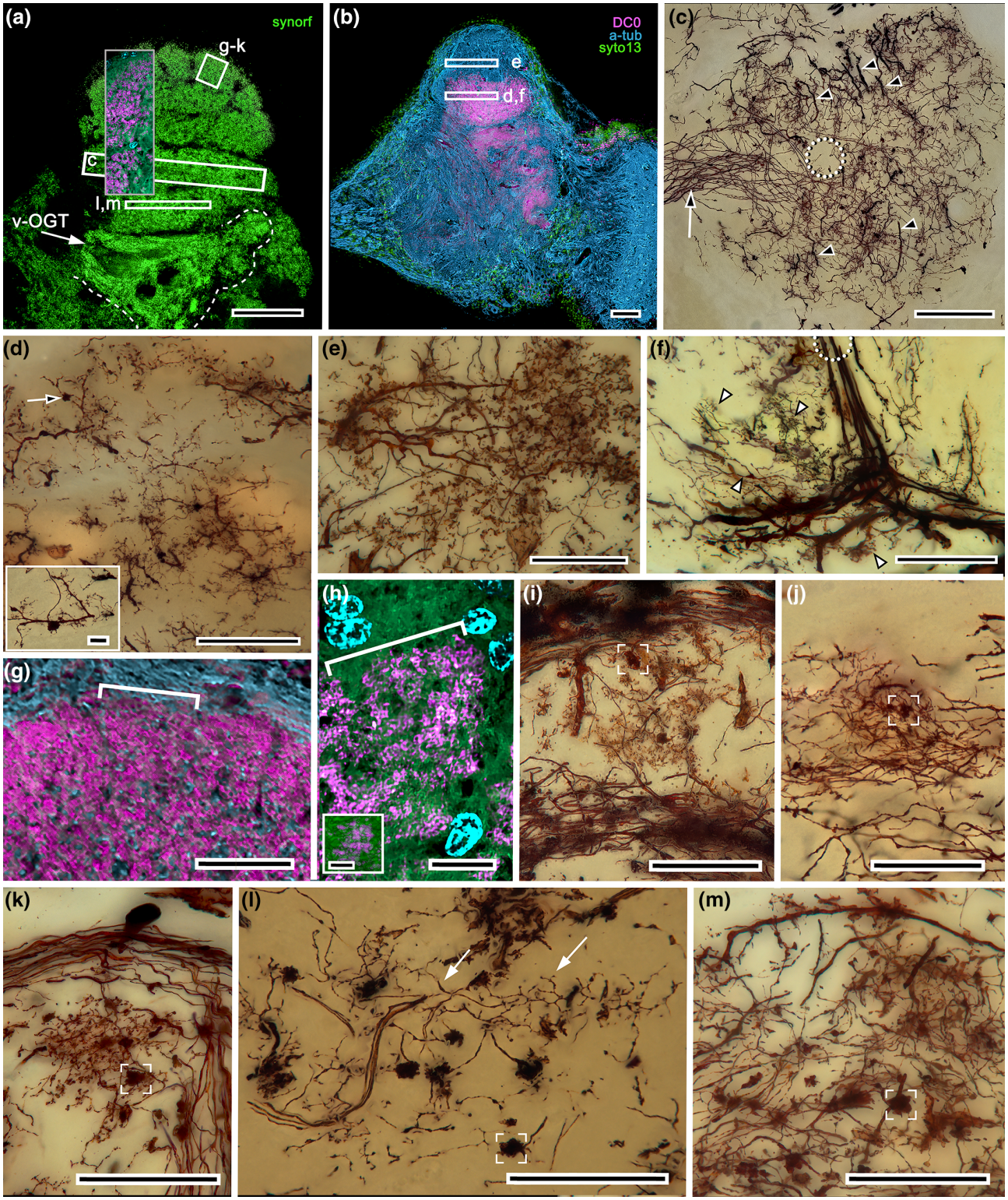

FIGURE 8 Legend on next page.

Whereas wide-field efferents from each neuropil of the hemiellipsoid body have been resolved through dye injection (McKinzie et al., 2003), Golgi impregnation appears to select different efferent morphologies. For example, tangentially directed dendrites equipped with exceptionally dense dendritic spines (Figure 8e) extend across large areas of the cupola neuropil. These efferent dendrites are distinct from those in the torus, which occur as discrete ensembles of tangentially directed processes, the branches of which are approximately aligned with the circumference of the neuropil. Axons of these efferent neurons exit the torus through its central core (Figure 8f).

Although it has not been possible to resolve any regular or repeat system of neurons in the torus, organization in the cupola suggests a system of synaptic complexes at its perimeter where its margin is thrown into folds and hillocks, as shown in Figure 8a,g,h. Labeling with antibodies against DC0 reveals the perimeter as a layer divided into discrete subunits that overlie a more uniform distribution of immunolabeled elements. The dimensions of these peripheral subunits, which are approximately rhomboidal, correspond to aggregates of neuropil that reveal affinity to antibodies raised against DC0 (Figure 8g) and delineated by synapsin immunolabeling and phalloidin staining (Figure 8h). These subunits further correspond to the width of velate glial cells at the margin of the cupola, immediately beneath incoming bundles of OGT terminals (Figure 8i). Bundles of processes from the OGT and their presynaptic boutons also appear to form discrete clusters, the dimensions of which match the arbors of local interneurons (Figure 8j,k). These rhomboidal units further match the lateral extent of intrinsic neuron dendrites illustrated in Figure 7c. Deeper in the cupola, systems of delicately branching and elongated processes (Figure 8l,m) suggest an arrangement of connections among intrinsic neuron terminals and larger tangential elements, possibly corresponding to neurons described by McKinzie et al. (2003).

5 | DISCUSSION

5.1 | Pagurus possesses the ancestral reptantian mushroom body

The "standard" hemiellipsoid body of reptantians, exemplified in Achelata and Astacidea, consists of two well-defined neuropils, either side by side or stacked one over the other, associated with globuli cells situated above and beside them (Sullivan & Beltz, 2001a, 2001b, 2004). As shown here in the crayfish *P. clarkii* and *O. immunis*, treatment with antibodies against α-tubulin or synapsin resolves some of their internal architecture, but nothing that immediately suggests discrete layered arrangements or specific territories other than those defined by incoming OGT axons and branches of large efferent neurons. It is only by using specific antibodies and Golgi impregnations that more detailed arrangements are resolved.

Immunocytological studies show a markedly different hemiellipsoid body in Coenobitidae, a member of the anomuran superfamily Paguroidea. In *Birgus latro* (the robber crab) and the Bermuda land crab *C. clypeatus*, the domed hemiellipsoid bodies are enormous denoted by their stratifications and dominating their lateral protocerebra (Krieger, Sandeman, Sandeman, Hansson, & Harzsch, 2010; Wolff et al., 2012). In *C. clypeatus*, the hemiellipsoid body comprises numerous anti-DC0 immunoreactive strata that Golgi impregnations and electron microscopy show contain orthogonal networks corresponding to those observed in the columnar mushroom body lobes of insects (Brown & Wolff, 2012; Wolff et al., 2012). This layered architecture is not unique to the hemiellipsoid body of Coenobitidae, however. Reduced silver and immunostainings of the squat lobster *Munida quadrispina*, a member of the anomuran superfamily Galatheoidea that shares a common ancestor with Paguroidea, also resolve comparable layers suggesting that these may be defining features of hemiellipsoid bodies across Anomura (Figure. 9).

FIGURE 8 Neuronal organization in the crayfish hemiellipsoid body. (a) Confocal scan through a depth of 4 μm of an antisynapsin labeled hemiellipsoid body showing best fit locations of areas depicting neurons in panels c, g–m. Furrows and hillocks define the surface of the cupola and distinguish its architecture from the torus beneath. Likewise, as shown in the vertical inset superimposed on these levels, synapsin-actin configurations tend to be larger in the torus. The ventral passage of olfactory globular tract axons (v-OGT) from the olfactory lobes terminates in the volume of neuropil (distal margin indicated by the dashed outline) immediately beneath the torus and clearly demarcated from the proximal margin of the torus. (b) Levels corresponding to panels d, e, (in cupola) and f (in torus) indicated in a specimen, in which anti-DC0 immunoreactivity occurred only in the torus and lateral protocerebral regions immediately beneath, including area VII. (c) Golgi impregnations showing OGT terminal fibers (at arrow) entering the proximal edge of the torus and intersecting large tangentially directed branches (arrowheads) of efferent neurons. (d) Top-down view of intrinsic neuron dendritic trees in the torus, notably broader than those of the cupola (Figure 7c). The inset shows a swollen OGT terminal in immediate contact with an intrinsic neuron dendrite (also at arrow in the main panel). (e) Wide-field dendritic arbor of an extrinsic (efferent) neuron extending across the cupola. Its dendrites are equipped with tuft-like tributaries richly decorated with postsynaptic spines. (f) The torus reveals ensembles of efferent neurons branching across its neuropil, the axons of which extend into the torus central core (half circle) en route to the lateral protocerebrum. Arrowheads indicate systems of densely branching local interneurons. (g) Detail showing large rectangular subunits highly immunoreactive to anti-DC0 that comprise the cupola's perimeter neuropil (location indicated in panel a). (h) Antisynapsin (magenta) and actin (green) demonstrating synaptic aggregates (enlarged in inset) within a volume corresponding to the DC0-positive subunits in panel g (both bracketed). (i) Perimeter neuropil of the cupola showing a glial domain, the dimensions of which correspond to DC0-positive subunits. (j) Converging OGT terminals (one bracketed) at a subunit in the cupula. (k) Local interneuron domain in a subunit of the cupola (terminal from OGT bracketed). (i) Diffuse and lengthwise extended local interneuron in the torus characterized by small collaterals (arrows) among swollen terminals from the OGT (bracketed). (m) Dense arrangements of large-diameter efferent neuron dendrites amongst OGT terminals (bracketed) and small diffusely arranged local interneuron processes. Scale bars = a, b, 100 μm; c-g, i–m, 50 μm; h, 25 μm, inset d, 10 μm; inset h, 2 μm

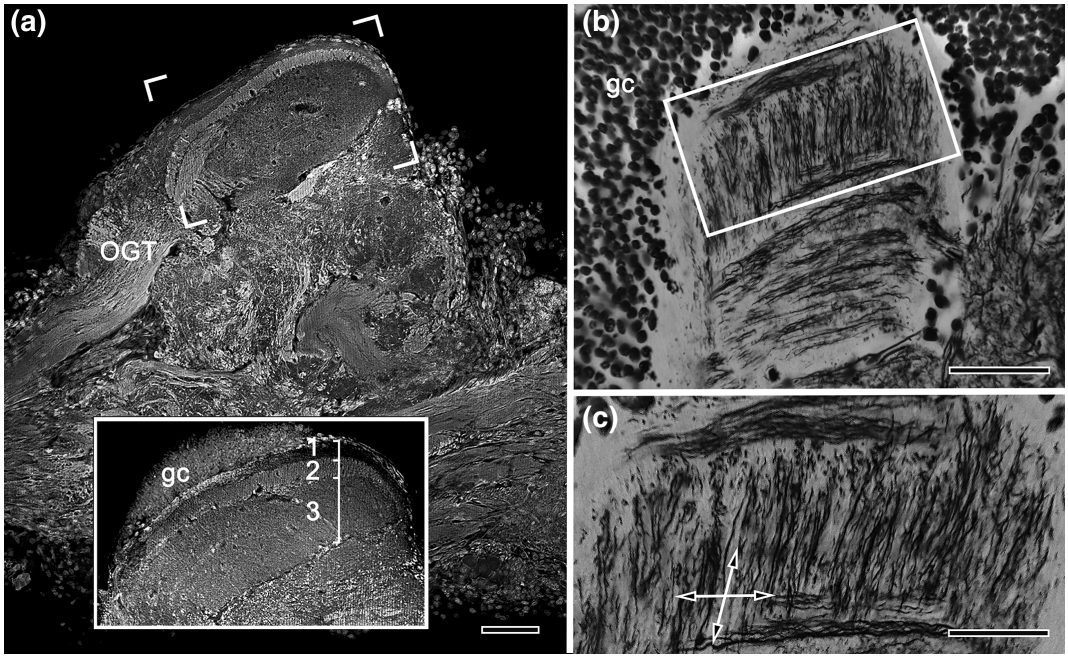

FIGURE 9 The galatheid *M. quadrispina* demonstrates features that characterize the calyces of *Pagurus* and the swollen hemiellipsoid bodies of *C. clypeatus*. (a) Anti-α-tubulin labeled lateral protocerebrum showing the OGT supplying the calyx (boxed), its layered organization (1, 2, 3 in inset) corresponding to that of *Pagurus* but entirely covered by the population of globuli cells (gc). (b). Reduced silver staining of sections cut tangential to the outer surface of the lateral protocerebrum resolves arrangements of neural processes in layer 3. (c) Enlargement of the boxed area in panel b showing the orthogonality of these arrangements (crossed arrows). These also typify the calyces of *Pagurus* and the multilayered hemiellipsoid body of *C. clypeatus* (Wolff et al., 2012). Scale bars = a, 100 μm; b, 50 μm; c, 25 μm

Coenobitidae diverged within Paguroidea (hermit and king crabs) approximately 35 million years ago, whereas marine hermit crabs represent an older lineage of Anomura, the superfamily Paguroidea. The greater age of Paguroidea may account for the retention of mushroom body characters, some of which are indistinct in the circuitry of *Coenobita* (Brown & Wolff, 2012), but which have been discovered in decapods and stomatopods that are outgroups to reptantians (Sayre & Strausfeld, 2019; Wolff et al., 2017). In *Pagurus*, such characters include a columnar lobe, the parallel fibers of which derive from systems of orthogonal networks in the calyces receiving their inputs from the OGT. *Pagurus* thus has the defining features of a mushroom body: calyx-like neuropils supplying axon-like processes to a columnar lobe (Farris, 2005; Strausfeld et al., 2009). The orthogonal networks in the pagurid calyces correspond to networks in strata of the coenobitoid hemiellipsoid body, and both are strongly immunoreactive to antibodies against DC0 (Brown & Wolff, 2012; Wolff et al., 2012).

In *Pagurus*, two adjoining calyces possess a population of intrinsic neurons, the extended processes of which terminate in the tubercular bulb of its columnar lobe. The shapes and arrangements of these intrinsic neurons are nearly identical to those of Kenyon cells, such as described for the cockroach *Periplaneta americana* and honey bee *Apis mellifera* mushroom bodies (Strausfeld, Homberg, & Kloppenburg, 2000; Strausfeld & Li, 1999a, 1999b). The spread of terminals from the OGT across intrinsic neuron dendritic trees is another feature that is typical of a mushroom body calyx. However, in *Pagurus*, it is a modified calyx, because it also possesses orthogonal arrangements of neurons that in an insect or a stomatopod occur in the columnar lobes. In *Pagurus*, circuits both in the calyces and the columnar lobes supply output neurons to the lateral protocerebrum. This is shown by the processes of 5HT- and TH-positive efferent neurons that align with circuits in the calyces (Figure 10a,f) or that extend among the intrinsic neuron endings in the bulbous terminal of the columnar lobe (Figure 2a).

Thus, as in *Drosophila* mushroom body lobes, aminergic efferent neurons lead off from corresponding networks of the *Pagurus* mushroom body. This elaborate center in *Pagurus* serves both as an integrator of sensory information and as a site where orthogonal networks perform higher level computations, as do circuits within the column of a lobed mushroom body. One of these functionalities is valence assessment, recognized as a cardinal property of the *Drosophila* mushroom body (Aso, Sitaraman, Ichinose, Kaun, et al. 2014; Cognigni et al., 2018). Might the corresponding center in a marine hermit crab also support valence assessment? A remarkable video recording (Bird, 2016) shows a marine hermit crab performing a behavior suggestive of self-awareness. After selecting a new shell and moving into it, the animal immediately transfers sea anemones adhering to its discarded residence onto corresponding positions of its new home. This action suggests a brain undertaking high-level assessments that result in actions that contribute to its survival.

5.2 | The hemiellipsoid body of *P. clarkii* is a modified mushroom body

Although differences between the lateral protocerebra of Astacidea and Anomura appear profound, there are nevertheless many corresponding features. Immunolabeling with antibodies against DC0,

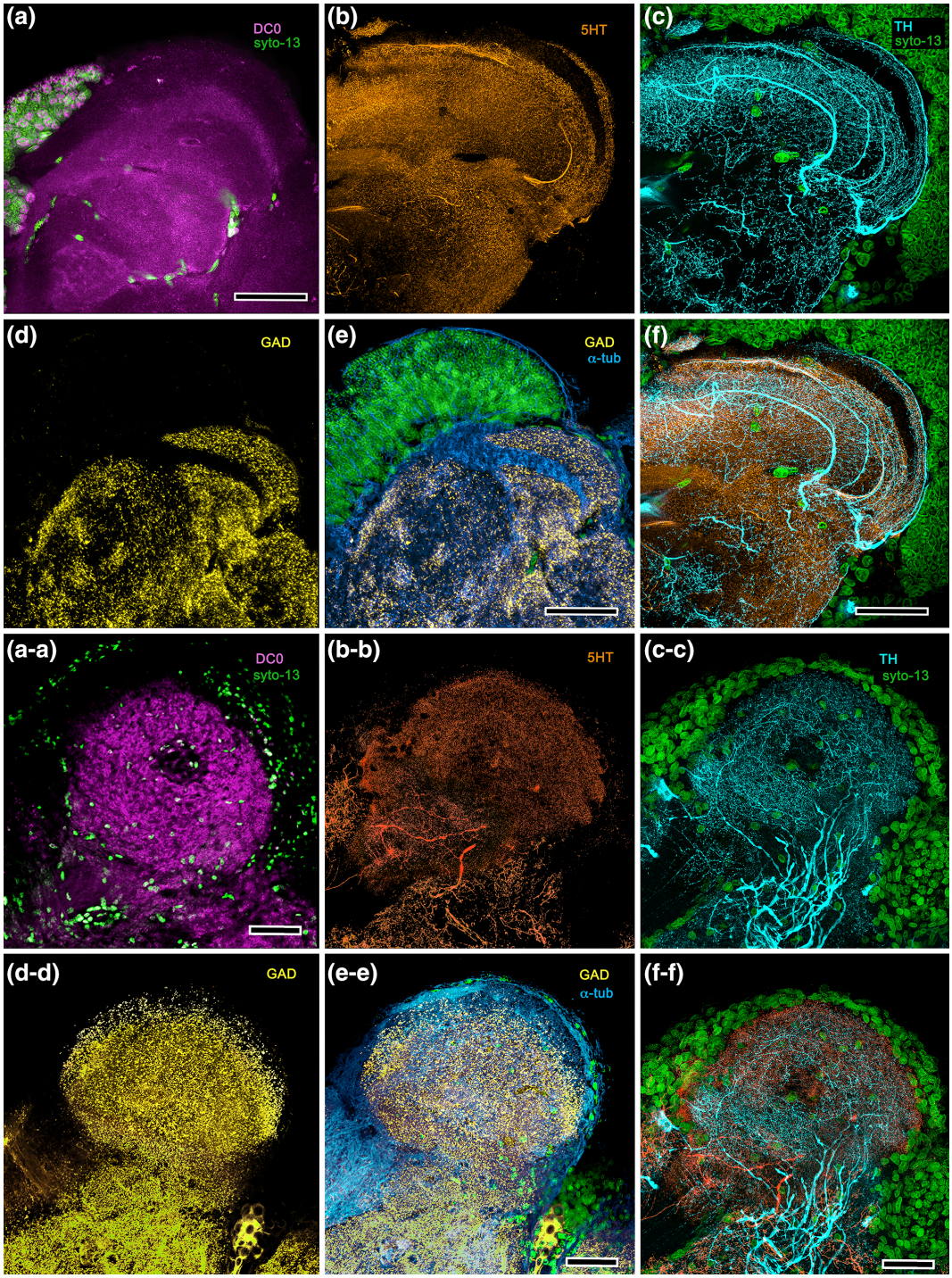

FIGURE 10 Comparisons of anti-DC0, -GAD, -5HT and -TH immunoreactivity in the *Pagurus* mushroom body and *Procambarus* hemiellipsoid bodies. (a-d) *Pagurus hirsutiusculus* mushroom body showing localized immunoreactivity to anti-DC0 (a), anti-5HT (b), and anti-TH (c). Anti-TH merged with anti-5HT in (f); and anti-GAD (d) merged with α-tubulin in (e). (a-a–f-f) Corresponding distributions in the hemiellipsoid body of *P. clarkii*. Scale bars in all panels = 100 μm

serotonin (5HT), TH, and GAD all illustrate the degree to which the organization of the mushroom body of the marine hermit crab matches that in the equivalent center in the crayfish, albeit reflecting a far less methodically arranged architecture (Figure 10). Whereas each of those antisera demonstrates in *Pagurus* a neuropil organized into neat layers, the same antisera resolve in *P. clarkii* a less ordered architecture. However, that this disorder is deceptive is shown by Golgi impregnations that reveal arrangements of intrinsic neurons, local circuits, and efferent systems contributing to discrete glomerulus-like territories.

It is also important to consider features that obviously differentiate the pagurid and astacid centers. These relate to attributes of the

reptantian lineage that includes Achelata and Astacidea, the brains of which are defined by enormous accessory lobes, approximately spherical neuropils serving as intermediate synaptic integrators between the olfactory lobes and the hemiellipsoid bodies (Sandeman et al., 1993; Sandeman, Beltz, & Sandeman, 1995; Wachowiak, Diebel, & Ache, 1996). The same lineages demonstrate that inputs to their hemiellipsoid bodies are supplied predominantly, in some genera exclusively, by the accessory lobes (Sullivan & Beltz, 2004, 2005). This contrasts with Paguridae where the two adjacent calyces receive their inputs from the olfactory lobes.

Lipophilic dye tracing showed that, although efferent neurons from the olfactory lobes extend to the lateral protocerebrum via the OGT in *P. clarkii*, these terminate mainly in neuropils beneath the hemiellipsoid body including volume "VII" identified by Blaustein et al. (1988). Applying fluorescent lipophilic dyes with different excitation spectra to the left and right accessory lobes, Sullivan and Beltz (2001a) further demonstrated that, whereas the cupola receives heterolateral inputs from both the ipsi- and contralateral accessory lobes, the torus receives input from the ipsilateral accessory lobe alone. The two neuropils of the crayfish hemiellipsoid were thus shown to be distinguished by different combinations of their afferent supply.

Calyx-like attributes of both the astacid cupola and torus are nevertheless suggested by their constituent interneurons: the assemblies of intrinsic neurons, local interneurons, glomerular complexes, and the subsequent arrangements of output neurons. Dendrites belonging to intrinsic neurons at the perimeter of the cupola contribute to localized territories that also involve amacrine-like local interneurons and converging axon terminals providing presynaptic boutons. The entire outer neuropil of the cupola, which is thrown into hillocks and depressions, appears to be composed of hundreds of these subunits, each defined by its affinity to the DC0 antibody. Immunocytology has ascribed a comparable subunit organization with the hemiellipsoid body of the marbled crayfish, *Procambarus virginalis* (Polanska, Yasuda, & Harzsch, 2007). Here, we show that in *P. clarkii*, presynaptic afferent specializations converge at a subunit in a manner comparable with the convergence of inputs carrying sensory information onto Kenyon cell dendrites in the insect mushroom body, an organization underlying the phenomenon of sparsening (Stopfer, 2014).

Intrinsic neurons in the cupola are comparable with neurons that in a mushroom body equipped with columnar lobes would provide parallel fibers to its lobe. In *P. clarkii*, the intrinsic neurons send their processes into deeper levels of the cupola, where they terminate among branches of wide-field output neurons, the axons of which leave the hemiellipsoid body through the core of the torus for destinations in the underlying lateral protocerebrum (McKinzie, Benton, Beltz & Mellon, 2003). The general organization of neurons in the torus appears to be similar, except that the morphologies of its constituent neurons are distinct from those in the cupola, particularly those that contribute to linear arrangements with local interneurons. The torus is also equipped with dendritic arbors of output neurons, which like those associated with the cupola are resolved by antibodies raised against TH (Figure 10c).

Earlier observations of fluorescent dye-filled output neurons demonstrated their origin from numerous cell bodies located ventrally in the lateral protocerebrum (McKinzie et al., 2003) and ascertained that their dendritic fields subtend extensive areas across each neuropil of the hemiellipsoid body, but not both. Erroneously suggested by us to correspond to large intrinsic neurons of the *Lebbeus* mushroom body (Sayre & Strausfeld, 2019), these efferent neurons in *P. clarkii* were proposed by their investigators to correspond physiologically to efferent neurons that originate from the lobes of insect mushroom bodies (McKinzie et al., 2003; Mellon, 2000, 2003; Li & Strausfeld, 1999).

Golgi impregnations indicate that neurons within the cupola do not extend to the torus, and vice versa. Thus, assuming that the neurons described by McKinzie et al. (2003) carry information independently from each of the hemiellipsoid body's neuropils, the conclusion—originally proposed by Sullivan and Beltz (2001b) from studies of the lobster hemiellipsoid body—is that each neuropil functions as a discrete and possibly independent integrator. If DC0 only occurs at detectable levels in centers that are undertaking active sensory associations, this may explain why in some crayfish preparations anti-DC0 immunoreactivity is revealed in the torus and not the cupola, or vice versa, or in both.

That there are two neuropils, one above the other in *P. clarkii* or adjacent in *P. argus* (Blaustein et al., 1988), suggests that doubling of these centers is a Leitmotif. In the lobster *Homarus americanus*, for example, the upper of the hemiellipsoid body's two neuropils partly enfolds the lower, hence receiving the name "cap" (Sullivan & Beltz, 2001a). Correspondence of the *Homarus* "cap" and the *Procambarus* cupola (neuropil II in Sullivan & Beltz, 2001a) is demonstrated by their corresponding relationship with the accessory lobes (Sullivan & Beltz, 2001b). This doubling appears to be shared by both reptantian and nonreptantian lineages: their higher order centers, with or without columnar lobes, generally comprise two or four units, each receiving terminals from the OGT (Sayre & Strausfeld, 2019; Sullivan & Beltz, 2004; Wolff et al., 2017). Even the diminutive lobeless hemiellipsoid body of the Dendrobranchiata, exemplified by *Penaeus duorarum*, comprises two distinct components (Sullivan & Beltz, 2004). Thus, the proposition here is that the cupola and torus are not part and parcel of a single modified mushroom body but are each independent centers; thus each a modified mushroom body, the ancestral condition being a quadri- or modified bipartite organization. In considering what may be the ancestral condition providing multiple components, the development of the insect mushroom body may be indicative. As shown for *Drosophila*, an insect mushroom body, when fully grown, comprises a quadripartite organization of glial and Kenyon cells, the lineages of which derive from four separate neuroblasts (Ito, Awano, Suzuki, Hiromi, & Yamamoto, 1997). This quadripartite organization is also seen in the stomatopod mushroom bodies although three members of the quartet have differently elaborated calyces, and the fourth member is calyxless (Wolff et al., 2017).

Another corresponding feature of the reptantian lateral protocerebrum that indirectly relates to the mushroom bodies is that, in insects, projection neurons from the olfactory lobes also provide major inputs to protocerebral neuropils, collectively termed the lateral

horn, disposed lateral to or beneath the mushroom bodies (Strausfeld, 1976; Tanaka, Awasaki, Shimada, & Ito, 2004). Terminals from the OGT of *P. clarkii* have similar dispositions, supplying thousands of endings to neuropils beneath the hemiellipsoid body (Sullivan & Beltz, 2001a, 2001b), as do terminals from the olfactory lobes in *Pagurus*.

5.3 | Efferent neurons suggest further homology

The astacid hemiellipsoid body has been described as containing exceptionally large dendritic trees of efferent neurons. These have been accorded the collective name "parasol cells" (McKinzie et al., 2003). The neurons integrate responses to multisensory stimulation and convey this information to other regions of the lateral protocerebrum (Mellon & Wheeler, 1999; Mellon, 2000). Various depictions of these neurons show significant neuroanatomical distinctions among them; these suggest five types denoted by their dendritic and terminal morphologies. Certain dye-coupled efferent neurons providing dendritic branches extending into the small hillocks of the cupola denote their likely inputs from circuits involving the cupola's intrinsic neurons (Mellon, Alones, & Lawrence, 1992). These efferent neurons, with collaterals extending into neuropil beneath the hemiellipsoid body (corresponding to Blaustein et al.'s area VII), have axons terminating as widely arborizing terminals in proximal neuropils of the lateral deutocerebrum. These neurons likely match one of the subsets of collateralized efferent neurons described by McKinzie et al. (2003). Another morphological type originating from cell bodies lateral to the hemiellipsoid body terminates as a highly restricted arborization in the lateral deutocerebrum (see Figure 10 in Mellon, Sandeman, & Sandeman, 1992). Its dendrites in the cupola are slender and diffuse, bearing no resemblance to efferent neurons depicted in Mellon et al. (1992) or efferent neurons equipped with enormous dendritic trees spreading through the entire cupola (Mellon, 2003).

The many types of local interneuron arrangements and the complex circuitry associated with intrinsic neurons provided by globuli cells demonstrate that the two hemiellipsoid neuropils retain some of the ground pattern elements of the ancestral mushroom body. This is further supported by one, or more usually both, neuropils showing affinity to the DC0 antibody, as do the columnar lobes of mushroom bodies. The recognition of corresponding aminergic systems in the mushroom bodies of Anomurans and hemiellipsoid bodies of Astacidea further supports the proposition that the reptantian hemiellipsoid body retains arrangements that derive from the ancestral mushroom body ground pattern. Figure 11 shows three possible steps, each suggested by a crown species, of the transformation of the ancestral mushroom body to that of a "standard" reptantian hemiellipsoid body.

5.4 | Has the "standard" hemiellipsoid body evolved twice?

Nonetheless unresolved issues remain, all of which address the question: which reptantian brain is the most derived? According to the

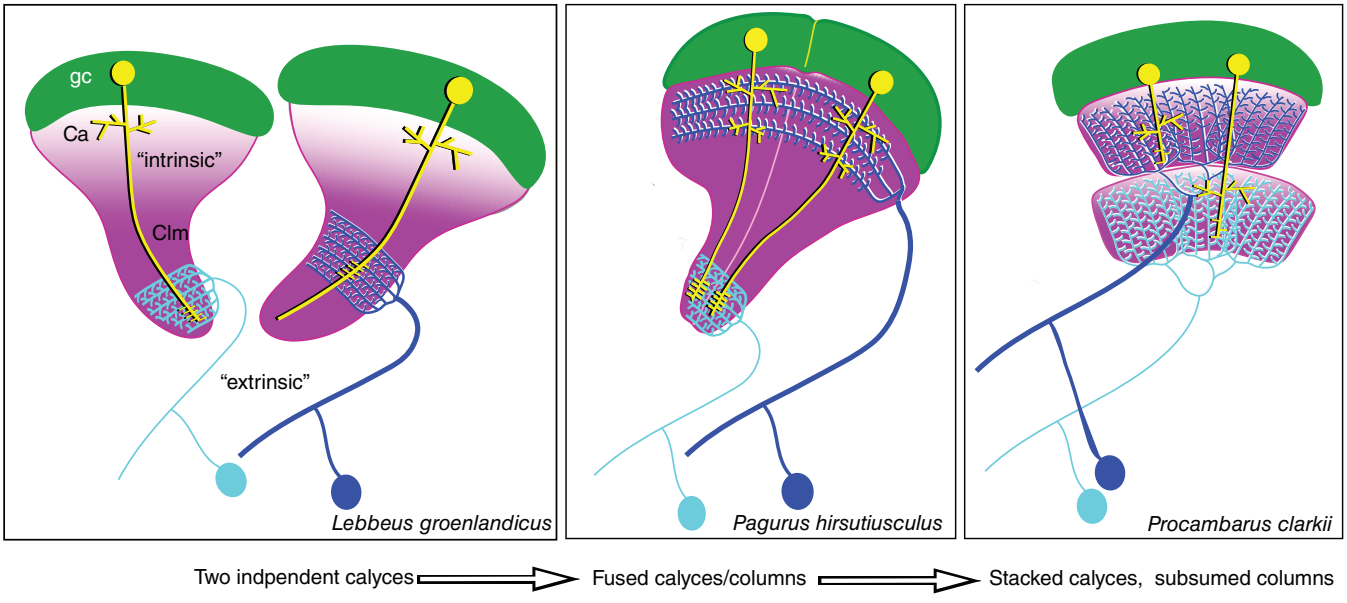

FIGURE 11 Proposed stages, each suggested by a crown species, of an evolved transformation of the ancestral mushroom body ground pattern to that of the "standard" reptantian hemiellipsoid body. In the first panel, the calyces and their columnar lobes of paired of mushroom bodies are shown as a gradually increasing magenta density reflecting affinity to anti-DC0; globuli cell clusters are green; intrinsic neurons yellow; efferent neurons cyan and blue. Inputs are omitted for clarity. All components in the mushroom body ground pattern, typified by the separated paired centers in *L. groenlandicus* (left panel) have corresponding modifications in the pagurid (center panel), where two mushroom bodies are fused and the calyces and lobes are immunoreactive to anti-DC0 throughout. The two separate neuropils of the astacid hemiellipsoid body (right panel) lack defined lobes, the circuits of which are incorporated into each neuropil. Both neuropils can show intense immunoreactivity to the DC0 antibody

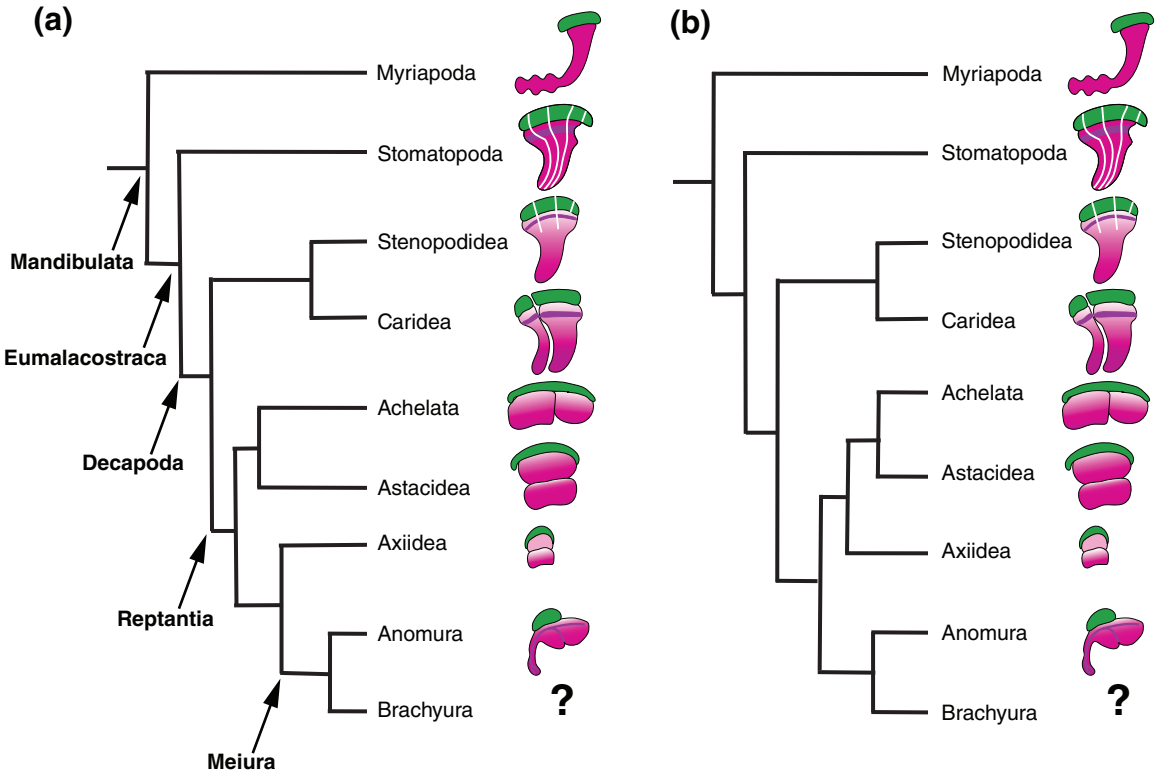

FIGURE 12 Attenuated phylogenies of Eumalacostraca (adapted from Wolfe et al., 2019) and its myriapod outgroup, showing scenarios of the divergence of the mushroom body ground pattern to paired dome-like centers within Reptantia, and the retention of its ancestral state in Anomura. The left cladogram (a), shows the sister relationship of Axiidea with Meiura and has the strongest support from molecular phylogeny. The alternative sister relations of Axiidea and Astacidea+Achelata (b) is also supported by molecular data but less strongly (Wolfe et al., 2019, and personal communication). The proposition that the mushroom body ground pattern in Anomura is ancestral is reinforced by its occurrence in Stenopodidea and Caridea, and in Stomatopoda. The proposition that the mushroom body ground pattern, denoted by a tubercular columnar lobe, is ancestral to Mandibulata is indicated by its presence in Myriapoda, the outgroup of total Pancrustacea (Wolff & Strausfeld, 2015). Mushroom bodies are indicated as quadripartite in Stomatopoda and Stenopodidea, and bipartite in Caridea and Anomura. Identification of a mushroom body homologue in Brachyura is unresolved [Color figure can be viewed at wileyonlinelibrary.com]

most recent decapod molecular phylogeny calibrated against the fossil record (Wolfe et al., 2019), Reptantia originated in the Devonian approximately 400 million years ago giving rise to diverging branches. One, providing the infraorders Achelata, Polychelida, and Astacidea, is defined neuroanatomically by its achelate and astacid members possessing the highly derived "standard" hemiellipsoid body morphologies (Sullivan & Beltz, 2004). These are supplied by the antennal globular tract carrying relays from extremely large accessory lobes in the deutocerebrum, which receive their primary inputs from the adjacent olfactory lobes. The accessory lobes are also connected to each other by a massive deutocerebral commissure (Sandeman & Scholtz, 1995). These attributes are absent from the other branch, two infraorders of which, Anomura and Brachyura, possess diminutive accessory lobes and, if they exist at all, indistinct commissures. In both infraorders, the antennal globular tract carries outputs predominantly from the olfactory lobes. But only in Anomura are many of the ancestral mushroom body characters resolved; unlike Brachyura, in which they are not.

Historically, the rationale for assuming that achelate/astacid brain organization denotes the reptantian (and malacostracan) ground pattern can be ascribed to the lack of evidence suggesting otherwise and lack of investigation of other lineages. The present account may correct that view. However, there are some remaining puzzles. Foremost among them is that the branch to which Anomura+Brachyura (together called Meiura) belong also includes the infraorders Gebiidea and Axiidea (Wolfe et al., 2019). These are the mud shrimps and ghost shrimps, the latter exemplified by Callianassidae (Wolfe et al., 2019). As shown by one representative species, *Neotrypaea californiensis*, brain organization in this family appears to match that typifying Astacidea and Achelata (Wolff et al., 2012). *Neotrypaea* possesses huge accessory lobes that, as in Achelata and Astacidea, are connected by a massive commissure. The accessory lobes provide outputs to the OGTs that branch to both lateral protocerebra where they supply some terminals to inconspicuous hemiellipsoid bodies. These centers comprise an outer glomerular neuropil, which is anti-DC0 negative, that surmounts a structurally distinct second volume that intensely labels with anti-DC0 (Wolff et al., 2012). Other than its DC0-immunonegative outer part, this organization of two stacked neuropils appears to conform to that in Astacidea. Would a phylogenetic tree of Reptantia be constructed based on neural characters

alone, these might not be able to resolve whether the astacid-callianassid hemiellipsoid body is ancestral or derived. Nevertheless, the anomuran mushroom body state is shared with the reptantian outgroups Caridea and Stenopodidea, and with the decapod outgroup Stomatopoda. Molecular analyses can suggest alternative relationships, in which Axiidea are not sister to Anomura+Brachyura (Figure 12a) but are sister to Astacidea+Achelata (Figure 12b). Thus, molecular data, albeit with a less optimal demonstration of molecular evolution, can support the mushroom body as representing the ancestral ground pattern (Figure 12; Wolfe et al., 2019, and personal communication).

Currently, however, Brachyura presents its own set of enigmas, not least of which is the difficulty of identifying precisely circumscribed hemiellipsoid bodies in this group. Instead, a center that corresponds morphologically and immunohistochemically to the stomatopod reniform body assumes morphological prominence (Wolff et al., 2017) and in Varunidae (shore crabs) serves as a habituating integrator of visual motion stimuli (Maza, Sztarker, Shkedy, Peszano, Locatelli, & Delorenzi, 2016).

ACKNOWLEDGMENTS

The research described here is supported by the National Science Foundation under Grant No. 1754798 awarded to NJS. We thank the staff of the University of Washington's Friday Harbor Laboratory, as well as Billie Swalla, Bernadette Holthuis, and Meegan Corcoran, for help in setting up research and for their advice. Our gratitude goes to Daniel Kalderon, Columbia University, New York, for supplying the DC0 antibody. This study has benefited from a collection of Golgi specimens of *P. hirsutiusculus* prepared on site at the Friday Harbor laboratory in 2012 by David Andrew, now at Lycoming College, Williamsport, PA. We have also profited from discussions with Gabriella Wolff (University of Washington), who read and commented on the manuscript as did Charles Derby (Georgia State University, Atlanta). Jo Wolfe (Harvard University) gave extensive advice regarding molecular phylogenies of Decapoda and how to consider them. Finally, we thank Camilla Strausfeld for critically discussing and meticulously editing the text.

DATA AVAILABILITY STATEMENT

Confocal images pertaining to this research are maintained on the investigators' storage devices. Immunostained specimens and Golgi-impregnated specimens are maintained in the Strausfeld laboratory at the Department of Neuroscience, University of Arizona.

ORCID

Nicholas J. Strausfeld https://orcid.org/0000-0002-1115-1774
Marcel E. Sayre https://orcid.org/0000-0002-2667-4228

REFERENCES

Andrew, D. R., Brown, S. M., & Strausfeld, N. J. (2012). The minute brain of the copepod *Tigriopus californicus* supports a complex ancestral ground pattern of the tetraconate cerebral nervous systems. *Journal of Comparative Neurology*, *520*, 3446–3470. https://doi.org/10.1002/cne.23099

Antonsen, B. L., & Paul, D. H. (2001). Serotonergic and octopaminergic systems in the squat lobster *Munida quadrispina* (Anomura, Galatheidae). *Journal of Comparative Neurology*, *439*, 450–468. https://doi.org/10.1002/cne.1362

Aso, Y., Sitaraman, D., Ichinose, T., Kaun, K. R., Vogt, K., Belliart-Guérin, G., et al. (2014). Mushroom body output neurons encode valence and guide memory based action selection in *Drosophila*. *eLIFE*, *3*, 1–42. https://doi.org/10.7554/eLife04580

Bellonci, G. (1882). Nuove ricerche sulla struttura del ganglio ottico della *Squilla mantis*. *Memorie Della Accademia Delle Scienze dell'Istituto di Bologna*, *4*, 419–426.

Bird, J. (2016). *Blue world*. British Broadcasting Corporation. https://www.youtube.com/watch?v=dYFALyP2e7U

Blaustein, D. N., Derby, C. D., Simmons, R. B., & Beall, A. C. (1988). Structure of the brain and medulla terminalis of the spiny lobster *Panulirus argus* and the crayfish *Procambarus clarkii*, with an emphasis on olfactory centers. *Journal of Crustacean Biology*, *8*, 493–519. https://doi.org/10.2307/1548686

Bracken-Grissom, H. D., Cannon, M. E., Cabezas, P., Feldmann, R. M., Schweitzer, C. E., Ahyong, S. T., … Crandall, K. A. (2013). A comprehensive and integrative reconstruction of evolutionary history for Anomura (Crustacea: Decapoda). *BMC Evolutionary Biology*, *13*, 128. https://doi.org/10.1186/1471-2148-13-128

Brauchle, M., Kiontke, K., MacMenamin, P., Fitch, D. H. A., & Piano, F. (2009). Evolution of early embryogenesis in rhabditid nematodes. *Developmental Biology*, *335*, 253–262. https://doi.org/10.1016/j.ydbio.2009.07.033

Brown, S., & Wolff, G. (2012). Fine structural organization of the hemiellipsoid body of the land hermit crab *Coenobita clypeatus*. *Journal of Comparative Neurology*, *520*, 2847–2863. https://doi.org/10.1002/cne.23058

Cognigni, P., Felsenberg, J., & Waddell, S. (2018). Do the right thing: Neural network mechanisms of memory formation, expression and update in *Drosophila*. *Current Opinion in Neurobiology*, *49*, 51–58. https://doi.org/10.1016/j.conb.2017.12.002

Cournil, I., Helluy, S. M., & Beltz, B. S. (1994). Dopamine in the lobster *Homarus gammarus*. I. Comparative analysis of dopamine and tyrosine hydroxylase immunoreactivities in the nervous system of the juvenile. *Journal of Comparative Neurology*, *334*, 455–469. https://doi.org/10.1002/cne.903440308

Crisp, K. M., Klukas, K. A., Gilchrist, L. S., Nartey, A. J., & Mesce, K. A. (2001). Distribution and development of dopamine- and octopamine-synthesizing neurons in the medicinal leech. *Journal of Comparative Neurology*, *442*, 115–129. https://doi.org/10.1002/cne.10077

Farris, S. M. (2005). Developmental organization of the mushroom bodies of *Thermobia domestica* (Zygentoma, Lepismatidae): Insights into mushroom body evolution from a basal insect. *Evolution & Development*, *7*, 150–159. https://doi.org/10.1111/j.1525-142X.2005.05017.x

Farris, S. M., & Sinakevitch, I. (2003). Development and evolution of the insect mushroom bodies: Towards the understanding of conserved developmental mechanisms in a higher brain center. *Arthropod Structure & Development*, *32*, 79–101 https://doi.org/10.1016/.

Farris, S. M., & Strausfeld, N. J. (2003). A unique mushroom body substructure common to basal cockroaches and to termites. *Journal of Comparative Neurology*, *456*, 305–320. https://doi.org/10.1002/cne.10517

Farris, S. M., & Van Dyke, J. W. (2015). Evolution and function of the insect mushroom bodies: Contributions from comparative and model

systems studies. *Current Opinion in Insect Science*, *12*, 19–25. https://doi.org/10.1016/j.cois.2015.08.006

Girard, C. F. (1852). A revision of the north American Astaci, with observations on their habits and geographic distribution. *Proceedings of Academy of Natural Sciences of Philadelphia*, *6*, 87–91.

Gronenberg, W. (2001). Subdivisions of hymenopteran mushroom body calyces by their afferent supply. *Journal of Comparative Neurology*, *436*, 474–489. https://doi.org/10.1002/cne.1045

Harzsch, S. (2004). Phylogenetic comparison of serotonin-immunoreactive neurons in representatives of the Chilopoda, Diplopoda, and Chelicerata: Implications for arthropod relationships. *Journal of Morphology*, *259*, 198–213. https://doi.org/10.1002/jmor.10178

Harzsch, S., Anger, K., & Dawirs, R. R. (1997). Immunocytochemical detection of acetylated α-tubulin and Drosophila synapsin in the embryonic crustacean nervous system. *International Journal of Developmental Biology*, *41*, 477–484.

Harzsch, S., & Hansson, B. S. (2008). Brain architecture in the terrestrial hermit crab *Coenobita clypeatus* (Anomura, Coenobitidae), a crustacean with a good aerial sense of smell. *BMC Neuroscience*, *9*, 58. https://doi.org/10.1186/1471-2202-9-58

Harzsch, S., & Waloszeck, D. (2000). Serotonin-immunoreactive neurons in the ventral nerve cord of Crustacea: A character to study aspects of arthropod phylogeny. *Arthropod Structure & Development*, *29*, 307–322. https://doi.org/10.1016/S1467-8039(01)00015-9

Ito, K., Awano, W., Suzuki, K., Hiromi, Y., & Yamamoto, D. (1997). The *Drosophila* mushroom body is a quadruple structure of clonal units each of which contains a virtually identical set of neurones and glial cells. *Development*, *124*, 761–771.

Kalderon, D., & Rubin, G. M. (1988). Isolation and characterization of *Drosophila* cAMP-dependent protein kinase genes. *Genes and Development*, *2*, 1539–1556. https://doi.org/10.1101/gad.2.12a.1539

Kenning, M., Müller, C., Wirkner, C. S., & Harzsch, S. (2013). The Malacostraca (Crustacea) from a neurophylogenetic perspective: New insights from brain architecture in *Nebalia herbstii* leach, 1814 (Leptostraca, Phyllocarida). *Zoologische Anzeiger - Journal of Comparative Zoology*, *252*, 319–336.

Klagges, B. R., Heimbeck, G., Godenschwege, T. A., Hofbauer, A., Pflugfelder, G. O., Reifegerste, R., … Buchner, E. (1996). Invertebrate synapsins: A single gene codes for several isoforms in *Drosophila*. *Journal of Neuroscience*, *16*, 3154–3165.

Krieger, J., Sandeman, R. E., Sandeman, D. C., Hansson, B. S., & Harzsch, S. (2010). Brain architecture of the largest living land arthropod, the Giant robber crab *Birgus latro* (Crustacea, Anomura, Coenobitidae): Evidence for a prominent central olfactory pathway? *Frontiers in Zoology*, *7*, 25. https://doi.org/10.1186/1742-9994-7-25

Krieger, J., Sombke, A., Seefluth, F., Kenning, M., Hansson, B. S., & Harzsch, S. (2012). Comparative brain architecture of the European shore crab *Carcinus maenas* (Brachyura) and the common hermit crab *Pagurus bernhardus* (Anomura) with notes on other marine hermit crabs. *Cell and Tissue Research*, *348*, 47–69. https://doi.org/10.1007/s00441-012-1353-4

Lange, A. B., & Chan, K. (2008). Dopaminergic control of foregut contractions in *Locusta migratoria*. *Journal of Insect Physiology*, *54*, 222–230. https://doi.org/10.1016/j.jinsphys.2007.09.005

Li, Y. S., & Strausfeld, N. J. (1999). Multimodal efferent and recurrent neurons in the medial lobes of cockroach mushroom bodies. *Journal of Comparative Neurology*, *409*, 647–663. https://doi.org/10.1002/(SICI)1096-9861(19990712)409:4<647::AID-CNE9>3.0.CO;2-3

Maynard, D. M., & Yager, J. G. (1968). Function of an eyestalk ganglion, the medulla terminalis, in olfactory integration in the lobster, *Panulirus argus*. *Zeitschrift für Vergleichende Physiologie*, *59*, 241–249.

Maza, F. J., Sztarker, J., Shkedy, A., Peszano, V. N., Locatelli, F. F., & Delorenzi, A. (2016). Context-dependent memory traces in the crab's mushroom bodies: Functional support for a common origin of high-order memory centers. *Proceedings of the National Academy of Science of the United States of America*, *113*, E7957–E7965. https://doi.org/10.1073/pnas.1612418113 PMID: 27856766.

McKinzie, M. E., Benton, J. J., Beltz, B. S., & Mellon, D., Jr. (2003). Parasol cells of the hemiellipsoid body in the crayfish *Procambarus clarkii*: Dendritic branching patterns and functional implications. *Journal of Comparative Neurology*, *462*, 168–179. https://doi.org/10.1002/cne.10716

McLaughlin, P. A., Komai, T., Lemaitre, R., & Listyo, R. (2010). Annotated checklist of anomuran decapod crustaceans of the world (exclusive of the Kiwaoidea and families Chirostylidae and Galatheidae of the Galatheoidea). Part I – Lithodoidea, Lomisoidea and Paguroidea. *The Raffles Bulletin of Zoology*, *23*, 5–107.

Mellon, D., Jr., Sandeman, D. C., & Sandeman, R. E. (1992). Characterization of oscillatory olfactory interneurons in the protocerebrum of the crayfish. *Journal of Experimental Biology*, *167*, 15–38.

Mellon, D., Jr. (2000). Convergence of multimodal sensory input onto higher-level neurons of the crayfish olfactory pathway. *Journal of Neurophysiology*, *84*, 3043–3055.

Mellon, D., Jr. (2003). Dendritic initiation and propagation of spikes and spike bursts in multimodal sensory interneuron: The crustacean parasol cell. *Journal of Neurophysiology*, *90*, 2465–2477. https://doi.org/10.1152/jn.00310.2003

Mellon, D., Jr. (2016). Electrophysiological evidence for intrinsic pacemaker currents in crayfish parasol cells. *PLoS One*, *11*, e0146091. https://doi.org/10.1371/journal.pone.0146091

Mellon, D., Jr., Alones, V., & Lawrence, M. D. (1992). Anatomy and fine-structure of neurons in the deutocerebral projection pathway of the crayfish olfactory system. *Journal of Comparative Neurology*, *321*, 93–111. https://doi.org/10.1002/cne.903210109

Mellon, D., Jr., & Wheeler, C. J. (1999). Coherent oscillations in membrane potential synchronize impulse bursts in central olfactory neurons of the crayfish. *Journal of Neurophysiology*, *81*, 1231–1241.

Nässel, D. R. (1988). Serotonin and serotonin-immunoreactive neurons in the nervous system of insects. *Progress in Neurobiology*, *30*, 1–85.

Polanska, M. A., Yasuda, A., & Harzsch, S. (2007). Immunolocalisation of crustacean-SIFamide in the median brain and eyestalk neuropils of the marbled crayfish. *Cell & Tissue Research*, *330*, 331–344. https://doi.org/10.1007/s00441-007-0473-8

Sandeman, D., Beltz, B., & Sandeman, R. (1995). Crayfish brain interneurons that converge with serotonin giant-cells in accessory lobe glomeruli. *Journal of Comparative Neurology*, *352*, 263–279. https://doi.org/10.1002/cne.903520209

Sandeman, D., & Scholtz, G. (1995). Ground plans, evolutionary changes and homologies in decapod crustacean brains. In O. Breidbach & W. Kutsch (Eds.), *The nervous systems of invertebrates: An evolutionary and comparative approach* (pp. 329–347). Basel, Switzerland: Birkhäuser.

Sandeman, D. C., & Luff, S. E. (1973). The structural organization of glomerular neuropile in the olfactory and accessory lobes of an Australian freshwater crayfish, *Cherax destructor*. *Zeitschrift für Zellforschung*, *142*, 37–61. https://doi.org/10.1007/BF00306703

Sandeman, D. C., Scholtz, G., & Sandeman, R. E. (1993). Brain evolution in decapod crustacea. *Journal of Experimental Zoology*, *265*, 110–133.

Sayre, M. E., & Strausfeld, N. J. (2019). Mushroom bodies in crustaceans: Insect-like organization in the caridean shrimp *Lebbeus groenlandicus*. *Journal of Comparative Neurology*, *2019*, 1–17. https://doi.org/10.1002/cne.24678

Schindelin, J., Arganda-Carreras, I., Frise, E., Kaynig, V., Longair, M., Pietzsch, T., … Cardona, A. (2012). Fiji: An open-source platform for biological-image analysis. *Nature Methods*, *9*, 676–682. https://doi.org/10.1038/nmeth.2019 PMID: 22743772.

Schmidt, M., & Ache, B. W. (1997). Immunocytochemical analysis of glomerular regionalization and neuronal diversity in the olfactory deutocerebrum of the spiny lobster. *Cell and Tissue Research*, *287*, 541–563.

Skoulakis, E. M. C., Kalderon, D., & Davis, R. L. (1993). Preferential expression in mushroom bodies of the catalytic subunit of protein kinase a

and its role in learning and memory. *Neuron*, *11*, 197–208. https://doi.org/10.1016/0896-6273(93)90178-T

Stemme, T., Iliffe, T. M., & Bicker, G. (2016). Olfactory pathway in *Xibalbanus tulumensis*: Remipedian hemiellipsoid body as homologue of hexapod mushroom body. *Cell and Tissue Research*, *363*, 635–648. https://doi.org/10.1007/s00441-015-2275-8

Stern, M. (2009). The PM1 neurons, movement sensitive centrifugal visual brain neurons in the locust: Anatomy, physiology, and modulation by identified octopaminergic neurons. *Journal of Comparative Physiology A*, *195*, 123–137. https://doi.org/10.1007/s00359-008-0392-5

Stieb, S. M., Muenz, T. S., Wehner, R., & Rössler, W. (2010). Visual experience and age affect synaptic organization in the mushroom bodies of the desert ant *Cataglyphis fortis*. *Developmental Neurobiology*, *70*, 408–423. https://doi.org/10.1002/dneu.20785

Stopfer, M. (2014). Central processing in the mushroom bodies. *Current Opinion in Insect Science*, *6*, 99–103. https://doi.org/10.1016/j.cois.2014.10.009

Strausfeld, N. J. (1976). *Atlas of an insect brain*. Berlin: Springer-Verlag.

Strausfeld, N. J. (2002). Organization of the honey bee mushroom body: Representation of the calyx within the vertical and gamma lobes. *Journal of Comparative Neurology*, *450*, 4–33. https://doi.org/10.1002/cne.10285

Strausfeld, N. J., Buschbeck, E. K., & Gomez, R. S. (1995). The arthropod mushroom body: Its roles, evolutionary enigmas and mistaken identities. In O. Breidbach & W. Kutsch (Eds.), *The nervous systems of invertebrates: An evolutionary and comparative approach* (pp. 349–381). Basel, Switzerland: Birkhaüser.

Strausfeld, N. J., Hansen, L., Li, Y., Gomez, R. S., & Ito, K. (1998). Evolution, discovery, and interpretations of arthropod mushroom bodies. *Learning and Memory*, *5*, 11–37.

Strausfeld, N. J., Homburg, U., & Kloppenberg, P. (2000). Parallel organization in honey bee mushroom bodies by peptidergic Kenyon cells. *Journal of Comparative Neurology*, *424*, 179–195. https://doi.org/10.1002/1096-9861(20000814)424:1<179::AID-CNE13>3.3.CO;2-B

Strausfeld, N. J., & Li, Y. S. (1999a). Representation of the calyces in the medial and vertical lobes of cockroach mushroom bodies. *Journal of Comparative Neurology*, *409*, 626–646. https://doi.org/10.1002/(SICI)1096-9861(19990712)409:4<626::AID-CNE8>3.0.CO;2-B

Strausfeld, N. J., & Li, Y. S. (1999b). Organization of olfactory and multimodal afferent neurons supplying the calyx and pedunculus of the cockroach mushroom bodies. *Journal of Comparative Neurology*, *409*, 603–625.

Strausfeld, N. J., Sinakevitch, I., Brown, S., & Farris, S. M. (2009). Ground plan of the insect mushroom body: Functional and evolutionary implications. *Journal of Comparative Neurology*, *513*, 265–291. https://doi.org/10.1002/cne.21948 PMID: 19152379.

Sullivan, J. M., & Beltz, B. S. (2001a). Neural pathways connecting the deutocerebrum and lateral protocerebrum in the brains of decapod crustaceans. *Journal of Comparative Neurology*, *441*, 9–22. https://doi.org/10.1002/cne.1394

Sullivan, J. M., & Beltz, B. S. (2001b). Development and connectivity of olfactory pathways in the brain of the lobster *Homarus americanus*. *Journal of Comparative Neurology*, *441*, 23–43. https://doi.org/10.1002/cne.1395

Sullivan, J. M., & Beltz, B. S. (2004). Evolutionary changes in the olfactory projection neuron pathways of eumalacostracan crustaceans. *Journal of Comparative Neurology*, *470*, 25–38. https://doi.org/10.1002/cne.11026 PMID: 14755523.

Sullivan, J. M., & Beltz, B. S. (2005). Integration and segregation of inputs to higher-order neuropils of the crayfish brain. *Journal of Comparative Neurology*, *481*, 118–126. https://doi.org/10.1002/cne.20346 PMID: 15558720.

Sullivan, J. M., Benton, J. L., Sandeman, D. C., & Beltz, B. S. (2007). Adult neurogenesis: A common strategy across diverse species. *Journal of Comparative Neurology*, *500*, 574–584. https://doi.org/10.1002/cne.21187

Tanaka, N. K., Awasaki, T., Shimada, T., & Ito, K. (2004). Integration of chemosensory pathways in the *Drosophila* second-order olfactory centers. *Current Biology*, *14*, 449–457. https://doi.org/10.1016/j.cub.2004.03.006

Thazhath, R., Liu, C., & Gaertig, J. (2002). Polyglycylation domain of β-tubulin maintains axonemal architecture and affects cytokinesis in Tetrahymena. *Nature Cell Biology*, *4*, 256–259. https://doi.org/10.1038/ncb764

Vogt, K., Aso, Y., Hige, T., Knapek, S., Ichinose, T., Friedrich, A. B., … Tanimoto, H. (2016). Direct neural pathways convey distinct visual information to *Drosophila* mushroom bodies. *eLIFE*, *5*, e14009. https://doi.org/10.7554/eLife14009

Wachowiak, M., Diebel, C. E., & Ache, B. W. (1996). Functional organization of olfactory processing in the accessory lobe of the spiny lobster. *Journal of Comparative Physiology A*, *178*, 211–226.

Wittfoth, C., Harzsch, S., Wolff, C., & Sombke, A. (2019). The "amphi"-brains of amphipods: New insights from the neuroanatomy of *Parhyale hawaiensis* (Dana, 1853). *Frontiers in Zoology*, *16*, 30. https://doi.org/10.1186/s12983-019-0330-0

Wolfe, J. M., Breinholt, J. W., Crandall, K. A., Lemmon, A. R., Lemmon, E. M., Timm, L. E., … Bracken-Grissom, H. D. (2019). A phylogenomic framework, evolutionary timeline and genomic resources for comparative studies of decapod crustaceans. *Proceedings of the Royal Society London B*, *286*, 20190079. https://doi.org/10.1098/rspb.2019.0079

Wolff, G., Harzsch, S., Hansson, B. S., Brown, S., & Strausfeld, N. (2012). Neuronal organization of the hemiellipsoid body of the land hermit crab, *Coenobita clypeatus*: Correspondence with the mushroom body ground pattern. *Journal of Comparative Neurology*, *520*, 2824–2846.

Wolff, G. H., & Strausfeld, N. J. (2015). Genealogical correspondence of mushroom bodies across invertebrate phyla. *Current Biology*, *25*, 38–44. https://doi.org/10.1016/j.cub.2014.10.049

Wolff, G. H., Thoen, H. H., Marshall, J., Sayre, M. E., & Strausfeld, N. J. (2017). An insect-like mushroom body in a crustacean brain. *eLIFE*, *6*, 1–24. https://doi.org/10.7554/eLIFE.29889

How to cite this article: Strausfeld NJ, Sayre ME. Mushroom bodies in Reptantia reflect a major transition in crustacean brain evolution. *J Comp Neurol*. 2020;528:261–282. https://doi.org/10.1002/cne.24752